tektonika

Impact of Salt Tectonics on Temperature Distribution Revealed by RSCM Thermometry in the SW Alps (France)

Naïm Célini *[1], **Jean-Paul Callot** [1], **Abdeltif Lahfid** [2], **Frédéric Mouthereau** [3]

[1]Université de Pau et des Pays de l'Adour, E2S UPPA, CNRS, Total, LFCR, Pau, France | [2]Bureau des Recherches Géologiques et Minières, Orléans, France | [3]GET, Université Paul Sabatier, Toulouse, France

Abstract Evaporites have a strong impact on the structural and sedimentary evolution of sedimentary basins and fold-and-thrust belts. They also have a thermal conductivity that can be more important than other sedimentary rocks and are thus able to modify the thermal history of these sedimentary basins and fold-and-thrust belts. Even though this property is known and has been of interest for the oil and gas industry, no field examples have been studied trying to decipher how salt rock impacts temperature distribution in fold-and-thrust belts. In this paper, we use the Raman Spectroscopy on Carbonaceous Material (RSCM) to track the record of the peak thermal event around three salt structures from the southern sub-Alpine fold-and-thrust belt in SE France. These three salt structures are (1) the Astoin allochthonous salt sheet and the associated overturned megaflap, (2) the Rocher de Hongrie and (3) the Daluis diapir. Our results show that the resulting record of peak temperatures around the structures is different depending on the type of salt structure and its kinematic. The Astoin structure shows that salt tectonics during the Jurassic-Cretaceous has impacted the temperature distribution around the allochthonous salt sheet while at Daluis and the Rocher de Hongrie, the temperatures have overprinted an already existing salt-related structure. The impact of the salt structure on temperature distribution is always local but the interpretation of the RSCM temperatures may systematically be difficult without considering early salt tectonics in the structural evolution of the area.

Executive Editor:
Gwenn Peron-Pinvidic
Associate Editor:
Berta Lopez-Mir
Technical Editor:
Mohamed Gouiza

Reviewers:
Laura Burrel
E. Izquierdo Lavall

Submitted:
4 August 2023
Accepted:
24 January 2024
Published:
6 March 2024

1 Introduction

The study of mountain building processes involves estimating the missing parts due to erosion. A classic workflow relies on the estimate of palaeotemperatures as a proxy for sedimentary and/or tectonic burial, associated to an estimate of its age. The tools often used to estimate palaeotemperatures are maturity indicators (Raman Spectroscopy on Carbonaceous Material – RSCM hereafter -, vitrinite reflectance, crystallinity of illite), fluid inclusions homogenisation temperatures, diagenetic and metamorphic mineralogy or isotopic equilibrium and low-temperature thermochronological analyses. The high thermal conductivity of salt rocks compared to surrounding sedimentary rocks (*Peterson and Lerche*, 1995; *Warren*, 2006; *Li et al.*, 2020) can have a local impact on the thermal field around salt structures in sedimentary basins (*Jensen*, 1983, 1990; *Vizgirda et al.*, 1985; *Mello et al.*, 1995; *Peterson and Lerche*, 1995; *Zhuo et al.*, 2016; *Davison and Cunha*, 2017; *Canova et al.*, 2018; *Cedeño et al.*, 2019; *Grunnaleite and Mosbron*, 2019; *Li et al.*, 2020). Generally, salt diapirs act as dipoles defined by a positive thermal anomaly at the top of the diapiric dome and a negative one beneath its stem. The anomalous temperatures measured in the sediments are either larger or lower than expected depending on their location on the flanks of the diapiric structure. The width and amplitude of thermal anomalies depends on the size of the structure and on their number. The geometry and the type of salt structures also affect the thermal regime around the structure. For instance, a columnar salt diapir provokes symmetrical thermal record in the surrounding depocenters. It is asymmetrical in case the structure is not columnar, especially if the diapir shows a salt overhang or feeds an allochthonous salt sheet. Mismatches between palaeotemperatures estimated from reconstructed burial histories and those measured are thus expected in natural geological environments involving salt-bearing rocks.

Salt rock is known to exert a strong control on the tectono-sedimentary evolution of sedimentary basins through halokinetic processes and acts as a decoupling level during both continental rifting

*✉ naim.celini@univ-pau.fr

and mountain building (*Davis and Engelder*, 1985; *Stewart et al.*, 1996; *Stewart and Clark*, 1999; *Cotton and Koyi*, 2000; *Withjack and Callaway*, 2000; *Costa and Vendeville*, 2002; *Bonini*, 2003; *Legeay et al.*, 2020). Depending on the regional tectonic regime, they are involved in various types of salt-related deformations including: (1) reactive salt tectonics due to extension (*Vendeville and Jackson*, 1992; *Nalpas and Brun*, 1993; *Jackson and Vendeville*, 1994; *Stewart and Clark*, 1999; *Dooley et al.*, 2005), (2) passive salt tectonics due to differential sediment loading (*Giles and Lawton*, 2002; *Giles and Rowan*, 2012; *Peel*, 2014; *Jackson and Hudec*, 2017; *Rowan and Giles*, 2021), (3) compressive salt tectonics in fold-and-thrust belts (*Davis and Engelder*, 1985; *Bonini*, 2003; *Brun and Fort*, 2004; *Hudec and Jackson*, 2006), and (4) strike-slip salt tectonics (*Sherkati and Letouzey*, 2004; *Koyi et al.*, 2008; *Cámara*, 2017; *Alsop et al.*, 2018). In compressional settings, salt tectonics influences the evolution of fold-and-thrusts belts by constituting vertical rheological heterogeneities (*Davis and Engelder*, 1985). These are preferential sites of shortening accommodation through squeezing, welding and favouring the nucleation of thrusts which will reach the shallower levels of the orogenic wedge (*Giles and Lawton*, 1999; *Rowan and Vendeville*, 2006; *Callot et al.*, 2007, 2012; *Jackson and Hudec*, 2017; *Duffy et al.*, 2018). They also control the distribution of folds (*Callot et al.*, 2012; *Fernandez and Kaus*, 2014) and can preserve the surrounding depocenters from the deformation (e.g. *Célini et al.*, 2020). In salt-detached accretionary prisms resulting from the inversion of depressed rift-related basins, the onset of topographic uplift may be delayed for several millions of years (*Jourdon et al.*, 2020). Numerous geological studies conducted in Western Europe have highlighted the importance of salt tectonics in the tectono-sedimentary evolution of fold-and-thrust belts including the Betics (*Flinch et al.*, 1996; *Berástegui et al.*, 1998; *Flinch and Soto*, 2017; *Pedrera et al.*, 2020), the Maestrat Basin (*Vergés et al.*, 2020), the Basque-Cantabrian Basin (*Poprawski et al.*, 2014, 2021; *Ducoux et al.*, 2019; *Cumberpatch et al.*, 2021; *Roca et al.*, 2021; *Ramos et al.*, 2022; *Miró et al.*, 2023), the Spanish Pyrenees (*McClay et al.*, 2004; *Lopez-Mir et al.*, 2014; *Burrel and Teixell*, 2021; *Hudec et al.*, 2021; *Gannaway Dalton et al.*, 2022; *Kalifi et al.*, 2023; *Pedrera et al.*, 2023), the French Pyrenees (*Canérot et al.*, 2005; *Ford and Vergés*, 2020; *Izquierdo-Llavall et al.*, 2020; *Labaume and Teixell*, 2020; *Motte et al.*, 2021), the Corbières in southern France (*Crémades et al.*, 2021; *Parizot et al.*, 2023), the Provence fold-and-thrust belt (*Bestani et al.*, 2016; *Espurt et al.*, 2019; *Wicker and Ford*, 2021), the Austrian Alps (*Schorn and Neubauer*, 2014; *Granado et al.*, 2019; *Strauss et al.*, 2021) and the external French Alps (*Gigot and Haccard*, 1970; *Emre*, 1977; *Graciansky et al.*, 1986; *Mascle et al.*, 1988; *Dardeau et al.*, 1990; *Dardeau and De Graciansky*, 1990; *Graham et al.*, 2012; *Célini et al.*, 2020, 2021, 2022; *Brooke-Barnett et al.*, 2023).

In the Western Alps, the role of Upper Triassic evaporites is known as acting as an efficient decollement level for thrust sheets in the Jura (*Philippe et al.*, 1998; *Sommaruga*, 1999), the southern Vercors (*Curnelle and Dubois*, 1986; *Philippe et al.*, 1998), the Diois-Baronnies derived from the Vocontian Domain (*Baudrimont and Dubois*, 1977; *Debrand-Passard et al.*, 1984) and the Digne Nappe system (*Arlhac and Rousset*, 1979; *Gidon et al.*, 1991a; *Faucher et al.*, 1988). In the SW Alps i.e., in the Vocontian Domain and the Digne Nappe systems, they are also known to have emplaced vertically through the sedimentary succession as diapiric structures (*Goguel*, 1939; *Lapparent*, 1940; *Emre*, 1977; *Emre and Truc*, 1978; *Perthuisot and Guilhaumou*, 1983; *Graciansky et al.*, 1986; *Kerckhove and Lereus*, 1986; *Mascle et al.*, 1986; *Kerckhove and Lereus*, 1987; *Mascle et al.*, 1988; *Dardeau and De Graciansky*, 1990; *Dardeau et al.*, 1990), these rocks were considered since then as second-order, impacting only locally the tectonics of the SW Alps. A series of recent studies have returned to the idea of the primary importance of salt by reinterpreting well-known structures of the SW Alps based on the most recent knowledge in salt tectonics (*Graham et al.*, 2012; *Célini et al.*, 2020, 2021, 2022; *Brooke-Barnett et al.*, 2023; *Csicsek*, 2023).

A recent reconstruction of the thermal history of the Mesozoic sediments transported in the southern sub-Alpine fold-and-thrust belt revealed that peak temperatures (Tmax) are inherited from pre-orogenic extensional phases during the Early-Middle Jurassic and Late Jurassic-Early Cretaceous rifting phases of the Alpine Tethys rather than due to Alpine orogeny (*Célini et al.*, 2023). During this pre-orogenic period, the whole passive margin was strongly affected by salt tectonics which could have affected, to an unknown extent, the record of temperature. To examine how salt tectonics could have impacted the temperature distribution during the Jurassic-Cretaceous thinning events, we provide 18 new RSCM Tmax in sediments sampled around salt structures identified in the sub-Alpine fold-and-thrust belt of the SW French Alps. Based on recent analysis of the Western Alps structural geology, we focus on three selected salt-related structures in the French sub-Alpine fold-and-thrust belt which are the Astoin diapir, the Rocher de Hongrie and the Daluis structure (Figure 1).

2 Geological Setting

2.1 Structural Framework

The European Alps result from the collision between Europe and Adria plates during the Late Cretaceous and the Cenozoic following the closure of the Alpine Tethys ocean that opened between the Early Jurassic and Early Cretaceous (*Lemoine et al.*, 1986; *Coward and Dietrich*, 1989; *de Graciansky et al.*, 2010; *Handy et al.*, 2010). Our study area is located in the external part of the SW branch of the Alpine orogen (Figure 1;

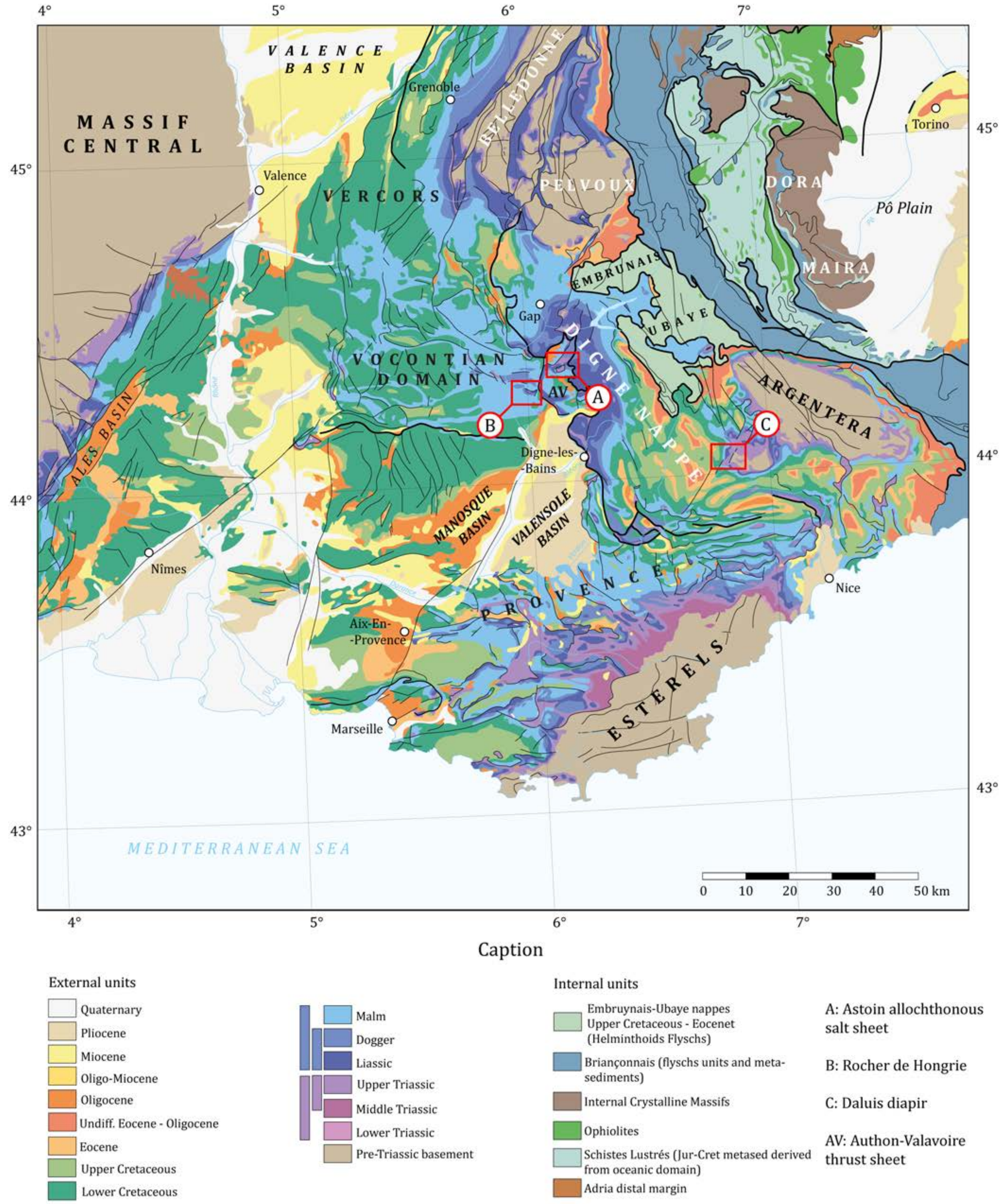

Figure 1 – Geological map of the SW Alps in SE France, modified from the BRGM French Geological Map at 1/1000000 (sheet South) (*Chantraine et al.*, 1996), with the location of the three salt structures studied in this paper: A = the Astoin allochthonous salt sheet, B = the Rocher de Hongrie and C = the Daluis diapir.

Chantraine et al., 1996), which originally constituted the sedimentary cover of the European rifted margin of the Alpine Tethys. The rifting responsible for the opening of the Alpine Tethys started in the Early Jurassic (Figure 2) (*Lemoine et al.*, 1986; *Dumont*, 1988; *Coward and Dietrich*, 1989; *de Graciansky et al.*, 1989) and lasted until ca. 165 Ma, i.e. the Bajocian which dates the oldest ophiolites rocks in the Western Alps (e.g. *Manatschal and Müntener*, 2009). As a result of continuous propagation of the southern North

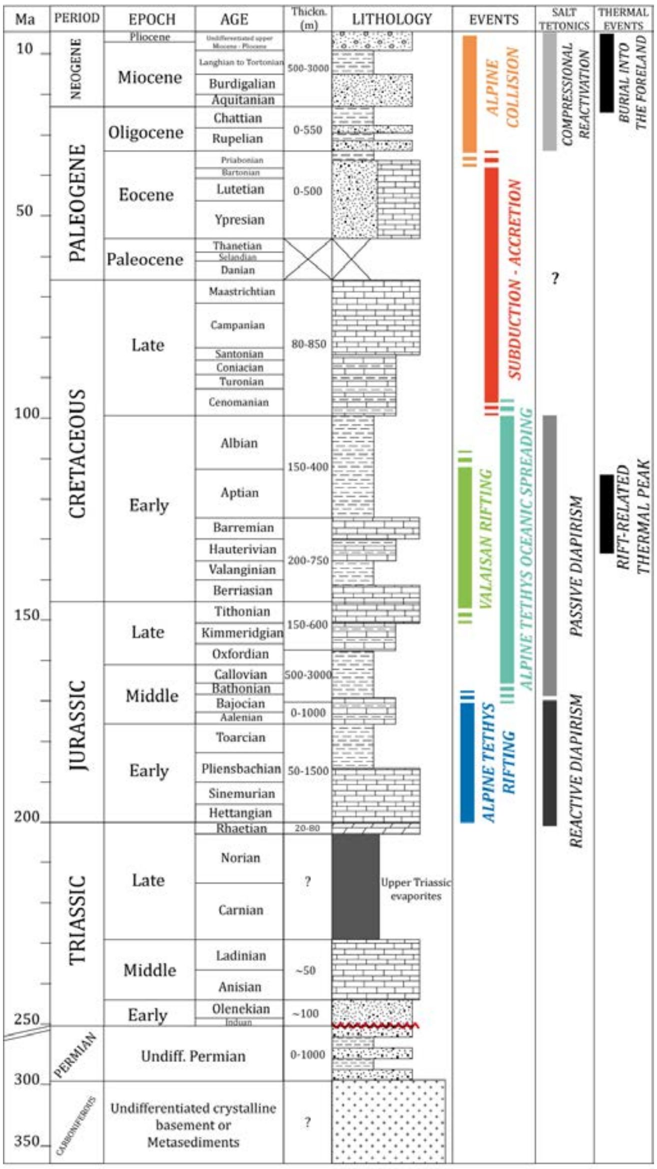

Figure 2 – Simplified stratigraphy of the SW Alps, from *Célini et al.* (2023). Thermal events from *Célini et al.* (2023) and salt tectonics phases from *Célini et al.* (2020, 2022).

Atlantic to the North, the European margin recorded reactivation of the previously rifted domains during the Late Jurassic – Early Cretaceous leading to the opening of the Valaisan Domain (*Stampfli and Borel*, 2002; *Liati et al.*, 2005; *Beltrando et al.*, 2007; *Loprieno et al.*, 2011), and in the Vocontian Domain of the SW Alps (*de Graciansky and Lemoine*, 1988; *Hibsch et al.*, 1992; *Angrand and Mouthereau*, 2021, see location in Figure 1). Oceanic spreading of the Alpine Tethys lasted until the Late Cretaceous when the subduction of the oceanic domain began in its eastern part, leading to the formation of the Alpine accretionary prism (e.g. *Coward and Dietrich*, 1989; *Handy et al.*, 2010). This Alpine accretionary prism migrated towards the N due to the convergence between Europe and Africa (*van Hinsbergen et al.*, 2020; *Le Breton et al.*, 2021). N-S directed shortening is occasionally recorded in the external units resulting either from (1) gravity gliding over the upper Bajocian – mid Oxfordian Terres Noires formation (Figure 2) during the Cretaceous in the Dévoluy (*Michard et al.*, 2010), (2) early salt tectonics in the Digne Nappe area during the Jurassic (e.g. *Célini et al.*, 2020) or (3) the N-S convergence between Europe and Africa during the Late Cretaceous–Paleogene (e.g. *Kley and Voigt*, 2008) which resulted in the propagation of the Pyrenean-Provence orogen to the S of the area (e.g. *Angrand and Mouthereau*, 2021) and to the N in the Pelvoux massif (*Vernet*, 1966; *Gidon*, 1979; *Ford et al.*, 1999; *Sue et al.*, 1997). From the Paleogene onwards, the convergence between Europe and Africa lead to two major compressional phases in the Western Alps, the first occurring between 50 and 34 Ma and the second one after 34 Ma (e.g. *Ford et al.*, 2006). The first stage represented N-NW-oriented propagation of the Alpine accretionary prism mainly recorded in the internal units (*Dumont et al.*, 2011, 2012). The second stage corresponds to the onset of collision in the SW Alps and resulted in crustal thickening and W-SW propagation of the deformation leading to the emplacement of the Embrunais-Ubaye flyschs nappes (during the Eocene-Oligocene, see location in Figure 1) and the Digne thrust system (from the Oligocene until the Late Pliocene) (*Gidon and Pairis*, 1986a, 1992; *Ford et al.*, 2006; *Kerckhove and Thouvenot*, 2010). The Digne thrust system, which forms the SW Alps thrust front, is constituted by three branches that are (1) the NNW-SSE main branch, called the Digne Nappe between the western termination of the Pelvoux crystalline massif to the N and the Barrême syncline to the S and containing a major thrust slice in its footwall, the Authon-Valavoire thrust sheet (Figure 1), (2) an E-W oriented branch called the Castellane Arc and (3) a NNW-SSE smaller branch called the Nice Arc to the SE. The Digne thrust system has carried a thick Mesozoic-Cenozoic cover towards the SW-SSW over a distance of 20-25 km (*Faucher et al.*, 1988; *Fry*, 1989; *Gidon and Pairis*, 1992; *Lickorish and Ford*, 1998; *Apps et al.*, 2004). The latest phase of thrusting of the Digne thrust system occurred during the Mio-Pliocene in relation with the Argentera basement block exhumation (*Gidon and Pairis*, 1992; *Apps et al.*, 2004; *Bigot-Cormier et al.*, 2006; *Ford et al.*, 2006; *Schwartz et al.*, 2017).

2.2 Stratigraphy

The main evaporite level involved in the Western Alps building was deposited during the Carnian-Norian (Late Triassic) prior to the onset of the Alpine Tethys rifting (e.g. *Haccard et al.*, 1989a). In a few locations, the so-called Muschelkalk limestones have deposited above a first evaporite level dated from the early Middle Triassic (*Campredon et al.*, 1980; *Brooke-Barnett et al.*, 2023). After the deposition of the Upper Triassic evaporites, the Triassic succession ends with the silts, limestones and dolostones from the Rhaetian, the total thickness of which varies between 20 and 80 m (*Rousset et al.*, 1983; *Dumont*, 1984; *Haccard et al.*, 1989a; *Arnaud et al.*, 1977; *Gidon et al.*, 1991b).

The Jurassic is composed by limestones and marls alternations (*Debrand-Passard et al.*, 1984) comprising at the base the calcareous Lower Jurassic (Hettangian - lower Pliensbachian) and the marly Lower Jurassic (upper Pliensbachian – Toarcian) (e.g. *Gidon*, 1997). The total thickness of the Lower Jurassic is highly variable, ranging from 50 to 1500m (*Gidon and Pairis*, 1986b; *Haccard et al.*, 1989a; *Gidon*, 1997; *Célini*, 2020; *Célini et al.*, 2020). The Lower Jurassic is overlain by the regular alternation of limestones and marls from the Aalenian-Bajocian stages. From the upper Bajocian to the mid-Oxfordian, the area has recorded an important phase of subsidence allowing the deposition of a thick black shale succession (between 500 and 3000m): the so-called "Terres Noires" formation (*Artru*, 1967, 1972; *Gidon*, 1971; *Baudrimont and Dubois*, 1977; *Gidon and Pairis*, 1986b). Then, the sedimentary succession was characterised by marls and limestones alternation during the upper Oxfordian and the Kimmeridgian with an increasing proportion of limestone upsection. This is followed by the massive limestone formation of the Tithonian which form characteristic cliffs in the sub-Alpine landscape. The whole thickness of the upper Oxfordian to the top Tithonian section ranges between 150 and 600m (e.g. *Baudrimont and Dubois*, 1977; *Debrand-Passard et al.*, 1984).

The Cretaceous begins with the massive limestone from the Berriasian, passing to the marls of the Valanginian, then to an alternation of limestones and marls during the Hauterivian, and the massive limestones from the Barremian (e.g. *Baudrimont and Dubois*, 1977; *Debrand-Passard et al.*, 1984). This section has a total thickness comprised between 200 and 750m. These are overlain by the second important black shales interval dated from the Aptian-Albian, 150 to 400 meters thick. The Late Cretaceous is globally made of an alternation of limestones and marls, from the Cenomanian to the Santonian, and then of massive limestones during the Campanian-Maastrichtian, for a total thickness of 80-850 meters depending on the location and on the amount of pre-Eocene erosion (e.g. *Baudrimont and Dubois*, 1977; *Debrand-Passard et al.*, 1984).

The only Paleocene deposits present in the area are the so-called "Helminthoid" flyschs from the Embrunais-Ubaye nappes (*Kerckhove and Thouvenot*, 2010). Otherwise, the Paleocene represents a general hiatus in the region, before the deposition of the first foreland deposits during the Eocene (*Baudrimont and Dubois*, 1977; *Debrand-Passard et al.*, 1984; *Coward and Dietrich*, 1989; *de Graciansky et al.*, 1989, 2010; *Ford et al.*, 1999). Eocene foreland sedimentation is generally represented by a succession of four formations that are (1) basal conglomerates, (2) the Nummulitic limestones, (3) the Globigerina marls and finally (4) the upper Eocene – lower Oligocene sandstones and conglomerates formations of the "Grès d'Annot" and the "Grès du Champsaur" (*Debrand-Passard et al.*, 1984; *Dardeau and De Graciansky*, 1990; *Gidon*, 1997; *Ford et al.*, 1999; *Fornel et al.*, 2004). The remaining part of the Oligocene is made of fluvial sandstones and continental red shales (*Haccard et al.*, 1989b; *Crumeyrolle et al.*, 1991; *Gidon and Pairis*, 1986b; *Ford and Lickorish*, 2004). In a few locations, these formations are now transported in the Digne Nappe and are thus in a piggy-back position (*Ford et al.*, 1999; *Apps et al.*, 2004; *Fornel et al.*, 2004). Younger foreland deposits (Mio-Pliocene) have deposited during the last stage of the foreland basin evolution, located in the Valensole basin. They are made of marine sandstones from the Aquitanian to the Tortonian and of continental conglomerates from the upper Miocene to the Late Pliocene (*Haccard et al.*, 1989a; *Crumeyrolle et al.*, 1991).

The presence and the thickness of the different units of the foreland succession is highly variable depending on the location and the stratigraphic level reached by erosion which varies laterally along-strike the belt. In the Valensole basin, the total thickness of the foreland deposits can locally reach 3 km (*Haccard et al.*, 1989a; *Crumeyrolle et al.*, 1991) and thermochronological data reveal that the depocenters that are at present-day in piggy-back positions could have reached 3 km of maximum thickness at the front of the Digne Nappe (see *Célini et al.*, 2023, for synthesis).

2.3 Salt Tectonics in the SW Alps

The SW Alps have been affected by widespread salt tectonics, related to the Upper Triassic evaporites, during their whole history since the Early Jurassic until the Mio-Pliocene (*Graciansky et al.*, 1986; *Kerckhove and Lereus*, 1986; *Mascle et al.*, 1986; *Dardeau and De Graciansky*, 1990; *Graham et al.*, 2012, 2019; *Célini et al.*, 2020, 2021, 2022; *Brooke-Barnett et al.*, 2023). Salt motion has started during the Early Jurassic triggered by regional extension (e.g. *Célini et al.*, 2020). Salt tectonics have been later maintained by the sedimentary load through passive diapirism during the whole Jurassic (e.g. *Célini et al.*, 2020), and in places during the Cretaceous (*Graham and Csicsek*, 2020; *Célini et al.*, 2021; *Brooke-Barnett et al.*, 2023) with possible effects of renewed extension during the later. Passive diapirism has led to the extrusion of allochthonous salt levels in various places during the deposition of the more shale-prone formations either during the Middle-Late Jurassic (*Graham et al.*, 2012; *Célini et al.*, 2020, 2021) or the Aptian-Albian (*Graham et al.*, 2019; *Graham and Csicsek*, 2020; *Brooke-Barnett et al.*, 2023). Inherited salt structures from the Mesozoic exerted a strong structural inheritance during orogeny by accommodating a substantial part of the shortening and preserving the surrounding depocenters from deformation (e.g. *Graham et al.*, 2012; *Célini et al.*, 2020). Syn-orogenic salt tectonics have also been evidenced in several locations during the Eocene-Oligocene (*Gigot and Haccard*, 1970; *Graham and Csicsek*, 2020; *Célini et al.*, 2021; *Brooke-Barnett et al.*, 2023) and until the Mio-Pliocene at the northern termination of the Valensole basin (*Célini et al.*, 2022).

2.4 Thermal Evolution of the External SW Alps

The thermal evolution of high-grade metamorphic rocks of the Western Alps has been widely investigated to quantify exhumation processes of subducted and underplated units of the Alpine accretionary wedge (*Gebauer et al.*, 1997; *Beyssac et al.*, 2002; *Carrapa et al.*, 2003; *Di Vincenzo et al.*, 2006; *Gabalda et al.*, 2009; *Angiboust et al.*, 2012, 2014; *Lanari et al.*, 2012; *Plunder et al.*, 2012; *Negro et al.*, 2013; *Schwartz et al.*, 2013; *Decarlis et al.*, 2017; *Manzotti et al.*, 2021; *Rosenberg et al.*, 2021; *Decrausaz et al.*, 2021; *Herviou et al.*, 2022). At the front of the Western Alps, in lower grade external units, thermochronology has been widely applied in the External Crystalline massif to decipher exhumation at upper crustal levels (*Bigot-Cormier et al.*, 2006; *Tricart et al.*, 2007; *Glotzbach et al.*, 2008, 2011; *Vernon et al.*, 2008; *Beucher et al.*, 2012; *Valla et al.*, 2012; *Schwartz et al.*, 2017; *Girault et al.*, 2022). Fluid inclusions were studied to apprehend the maximum burial reached in the Vocontian Domain (*Perthuisot and Guilhaumou*, 1983; *Guilhaumou et al.*, 1996). A few studies were focused on the estimation of eroded syn-orogenic deposits or internal units that have overthrusted the external units during orogeny using thermochronology on clastic deposits (*Labaume et al.*, 2008; *Jourdan et al.*, 2013; *Schwartz et al.*, 2017), vitrinite reflectance (*Deville and Sassi*, 2006) or the RSCM approach (*Bellanger et al.*, 2015; *Boutoux et al.*, 2016; *Girault et al.*, 2020; *Balansa et al.*, 2023). A recent study using the RSCM approach and basin modelling evidenced a thermal inheritance of the rifting phases highlighting that the peak temperatures have not been overprinted during the orogeny (*Célini et al.*, 2023) such as proposed in the internal units of the Maritime Alps (*Decarlis et al.*, 2017). The tectono-sedimentary evolution of the external SW Alps thus reveals that RSCM Tmax achieved by the rocks were attained during two thermal events. The first one occurred during the rifting events related to the Alpine Tethys and Valaisan Domain openings, respectively during the Early-Middle Jurassic and the Late-Jurassic Early Cretaceous. The maximum lithospheric thinning attained during the Early Cretaceous is responsible for the high Tmax (250-330°C) observed in the Jurassic rocks. The second thermal event occurred during the Cenozoic orogeny and corresponds to the burial of the Digne Nappe in the Alpine foreland prior to its emplacement. This event is responsible for the calculated Tmax of about 100-150°C recorded in the Cretaceous and Cenozoic rocks, but it has not overprinted those of the Jurassic rocks beneath (*Célini et al.*, 2023). Several observations indicate the occurrence of an inherited rift-related thermal event such as: (1) the temperature gap between the Digne Nappe and the overlying NW part of the Embrunais-Ubaye thrust sheets showing a ~100°C temperature drop, (2) the impossibility to reproduce the higher temperatures at the front of the Digne Nappe with a classical geothermal gradient of 30°C/km because they imply a 6-7 km-thick section of syn-orogenic deposits while thermochronological data testify for a maximum thickness of 3 km for syn-orogenic strata at the front of the nappe (*Jourdan et al.*, 2013; *Schwartz et al.*, 2017), (3) the presence of two temperature trends along vertical sections with a 50-100°C shift between the two trends requiring the development of two geothermal gradients (*Célini et al.*, 2023).

3 Salt Structures in the Sub-Alpine Fold-and-Thrust Belt

3.1 The Astoin Allochthonous Salt Sheet and the Overturned Megaflap

The Astoin diapiric complex (Figure 3) is located in the Authon-Valavoire thrust sheet and presents a complex structure that strongly varies laterally (*Célini et al.*, 2020, 2021). Diapiric activity has started during the Early Jurassic rifting, which triggered reactive diapirism as testified by the major growth strata observed during the Sinemurian (Figure 3C) (*Célini et al.*, 2020). In places, the great thickness of the original evaporite mother layer favoured passive diapirism coeval with the rifting, such as at the location of the Astoin megaflap. Later, the diapirism continued through passive diapirism, the deposits were not able to cover the whole diapir allowing in places the inflation of the salt structure and the progressive overturning of the diapir flank associated to salt extrusion at the seafloor during the Bajocian, in the eastern part of the diapiric complex forming an overturned megaflap (Figure 3) (*Célini et al.*, 2020, 2021). Locally, the diapir has preserved pieces of carapace such as the Grande Gautière (Figure 3A) (*Célini et al.*, 2020, 2021). The development of the allochthonous salt sheet took place until the Aptian-Albian (*Célini et al.*, 2021), just after the main thermal event affecting the Jurassic and Lower Cretaceous strata in the external SW Alps (*Célini et al.*, 2023). Here we focus on the thermal evolution of the Astoin diapiric complex in its eastern part at the location of the overturned megaflap.

3.2 The Rocher de Hongrie Megaflap

The Rocher de Hongrie is a structure located in the easternmost part of the Vocontian basin, in the footwall of the Authon-Valavoire thrust sheet (Figure 4A). It consists of a NW-SE-oriented panel of Lower Jurassic rocks, forming an easily recognisable hill in the relatively flat landscape of that part of the Vocontian Domain, essentially constituted by the "Terres Noires" formation in that area (Figure 4B). It has been interpreted as a faulted anticline (*Gidon et al.*, 1991a) even though *Mascle et al.* (1986) have mentioned a possible salt-related origin. An elongated NW-SE outcrop of Upper Triassic evaporites is located in the core of the anticline-like structure (Figure 4B). These evaporites

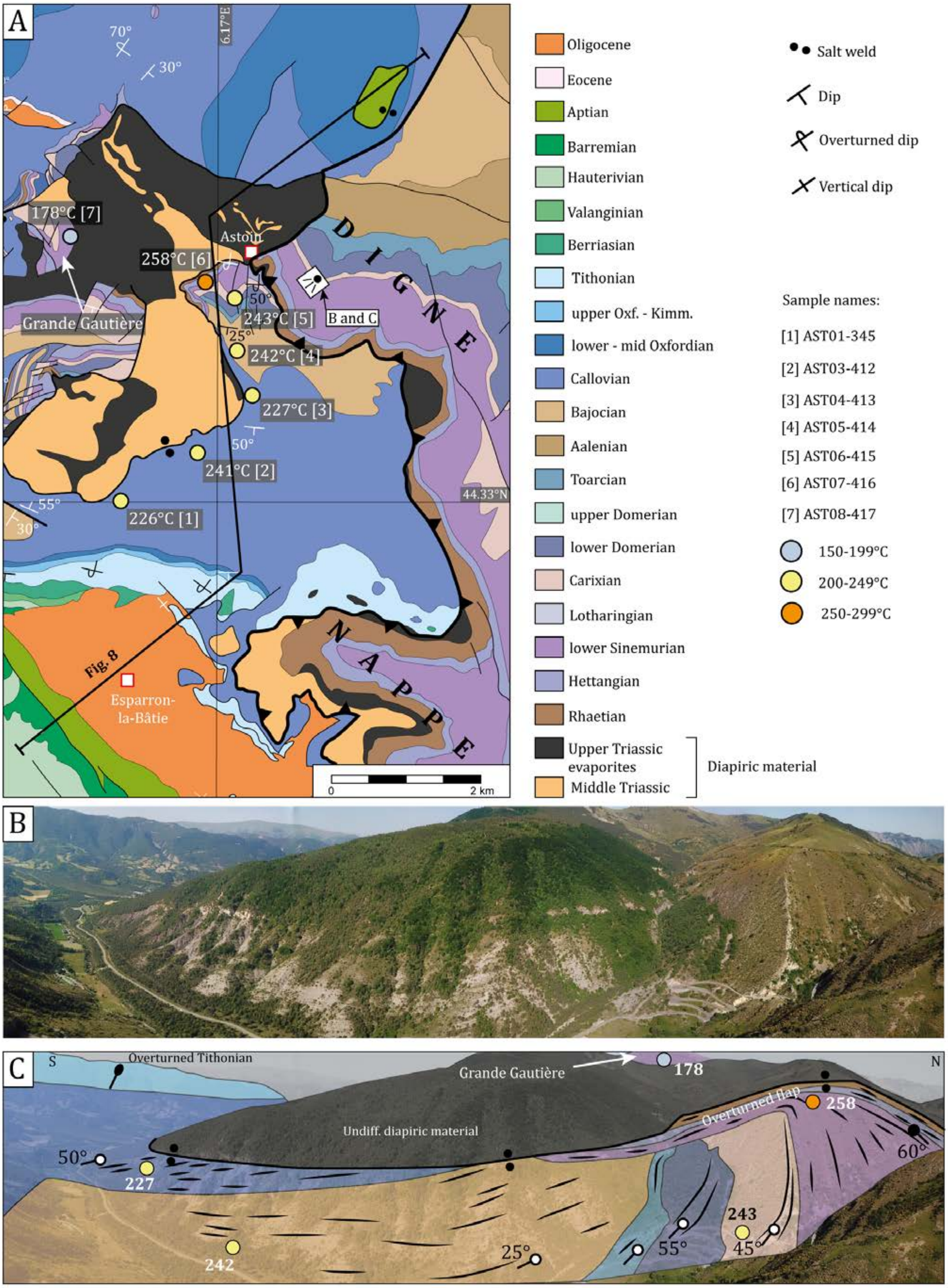

Figure 3 – **A:** Geological map of the Astoin area, modified from the BRGM geological map at 1/50000 (sheet Seyne) (*Arlhac et al.*, 1983). **B:** Uninterpreted and **C:** interpreted panorama of the Astoin overturned flap (from *Célini et al.*, 2021). See location in A. Temperatures are given in °C.

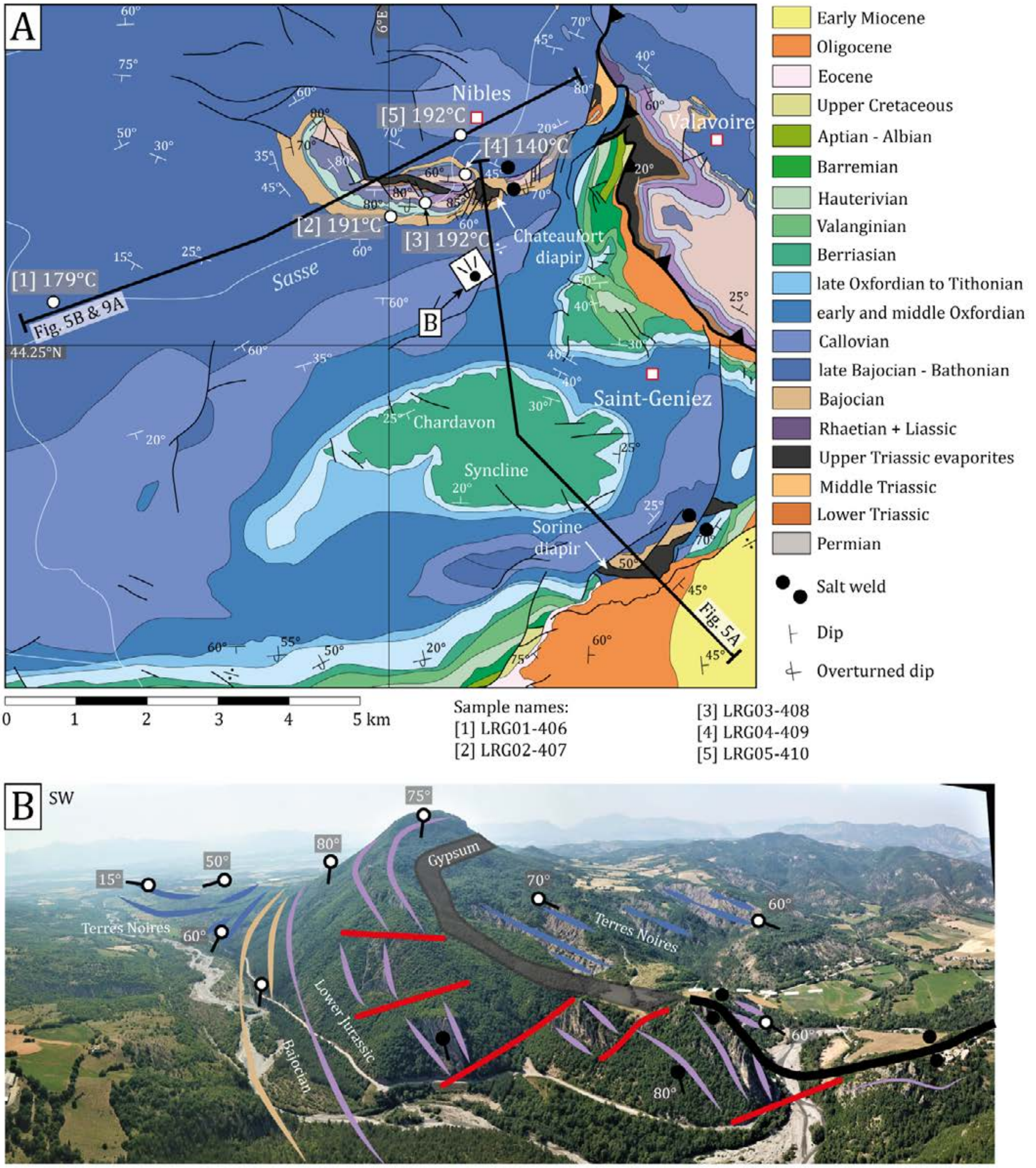

Figure 4 – **A:** Geological map of the Rocher de Hongrie area, modified from the BRGM geological map at 1/50000 (sheets Sisteron) (*Gigot et al.*, 2013). **B:** Panorama of the Rocher de Hogrie. Temperatures given in °C. See location in A.

are in direct contact with successive stratigraphic units of the Jurassic and the Rocher de Hongrie laterally correlates with a known salt structure (*Gigot et al.*, 2013): the Chateaufort diapir (Figure 4A, Figure 5A).

On the southern side of the structure, the Lower Jurassic rocks from the panel lie conformably over the evaporites and are dipping between 80° towards the SW and 80° overturned towards the NE. The dips in the Middle Jurassic rocks abruptly decrease to 35-45° towards the SW and 60° towards the S depending on the location (Figure 4A). Normal faults are affecting the Lower Jurassic and the Middle Jurassic in the vertical panel. These are sealed by the Bajocian or the Terres Noires formation and root into the evaporites. Many internal unconformities are also observable in map view (Figure 4A). Indeed, the Aalenian is systematically missing, and the

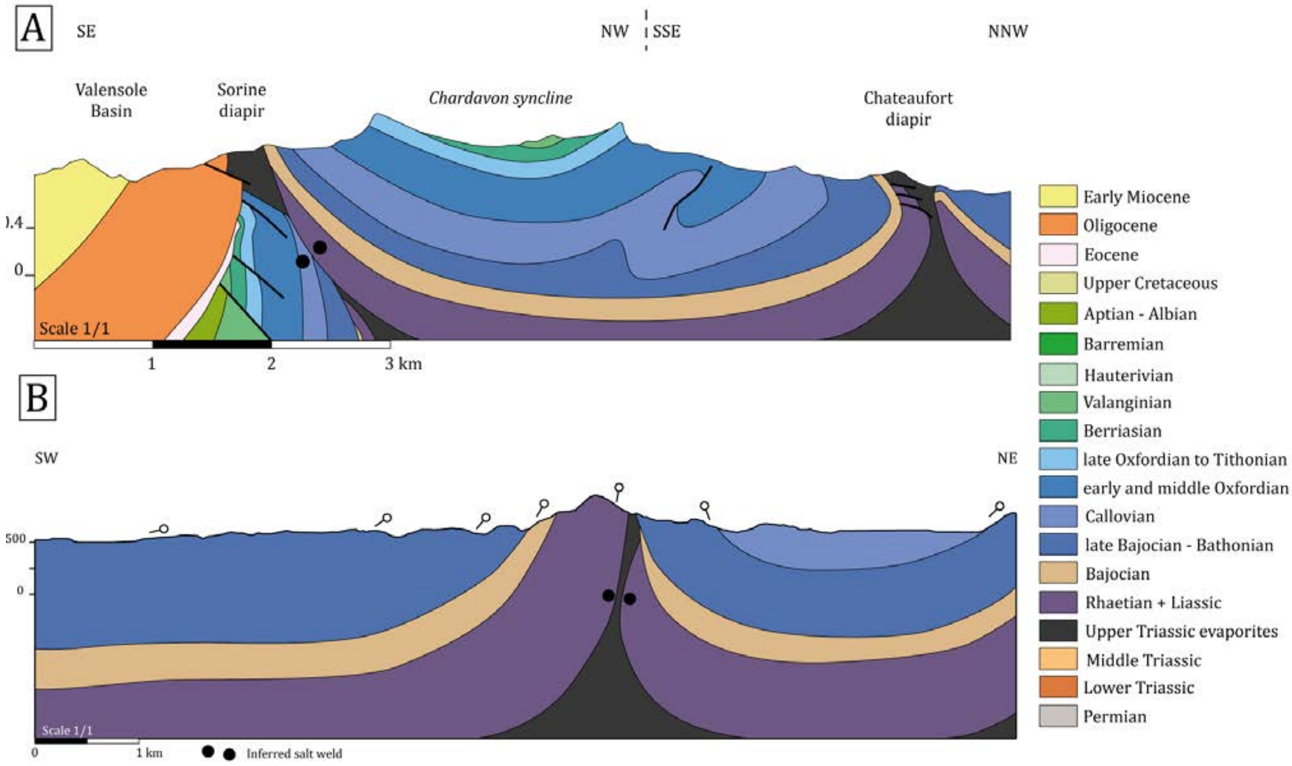

Figure 5 – **A:** Cross-section through the Sorine and Chateaufort diapir, redrawn from Gigot et al. (2013). **B:** Cross-section through the Rocher de Hongrie. See locations of the sections in Figure 4.

Bajocian lies over different stages of the Lower Jurassic also affected by internal unconformities (Figure 4A). On the northern edge, the evaporites are in abnormal contact with various stages of the Jurassic spanning from the Lower Jurassic to the Terres Noires formation. These strata abut against the evaporites and dip 60-70° towards the NNW-NW (Figure 4).

This asymmetric setting on both sides of evaporites outcrops is common of salt-related structures especially with the rocks from the northern edge, abutting against these evaporites and testifying for a syn-sedimentary salt flow (e.g. *Jackson and Hudec*, 2017). The strata from the southern edge forming a sub-vertical panel show in cross-section a megaflap-like structure such as defined by *Rowan et al.* (2016) (Figure 5B). Thus, we propose that the Rocher de Hongrie is a megaflap adjacent to a salt structure that initiated during the Lower Jurassic in response to regional extensional event as evidenced by the normal faults affecting the syn-rift strata only (Figure 4). Later, salt flow might have been maintained by passive diapirism during the Middle Jurassic passive margin stage such as for other structures of the SW Alps (*Graciansky et al.*, 1986; *Dardeau and De Graciansky*, 1990; *Célini et al.*, 2020). It is likely that the Rocher de Hongrie and the Chateaufort evaporites formed in fact a single continuous salt wall that has been squeezed during the Alpine compression. This interpretation is supported by the fact that the Rocher de Hongrie is aligned with diapirs of the area of Laragne-Montéglin, Upaix and Lazer a few kilometres to the NW (Figure 1), following a NW-SE trend, probably similar to those of normal faults affecting the basement beneath the evaporites during the Jurassic (*Mascle et al.*, 1988; *Gidon et al.*, 1991a).

3.3 The Daluis Diapir

The Daluis diapir is located to the SW termination of the Dôme de Barrot (Figure 1), which is a Permian half-graben inverted during the Alpine orogeny (e.g. *Apps et al.*, 2004). In this location of the SW Alps, two evaporites levels are observed, one beneath the Middle Triassic limestones from the Muschelkalk formation and one above it (*Campredon et al.*, 1980). The activity of the Daluis diapir began during the Lower Jurassic by reactive diapirism, followed by a passive phase of diapirism until the end of the Jurassic (*Dardeau and De Graciansky*, 1990; *Brooke-Barnett et al.*, 2023). The Mesozoic and Cenozoic stratigraphy of the area shows a global growth strata (Figure 6) but the main phase of differential accommodation due to salt motion has been recorded during the Jurassic testifying for a main diapiric phase at that time (*Dardeau and De Graciansky*, 1990; *Brooke-Barnett et al.*, 2023). During the Aptian-Albian, the evaporites have been extruded at the seafloor a few kilometres farther to the S forming an allochthonous salt sheet (*Brooke-Barnett et al.*, 2023). If salt evacuation has migrated farther south, it probably explains why the Daluis diapir has not recorded a significant diapiric activity during the Cretaceous.

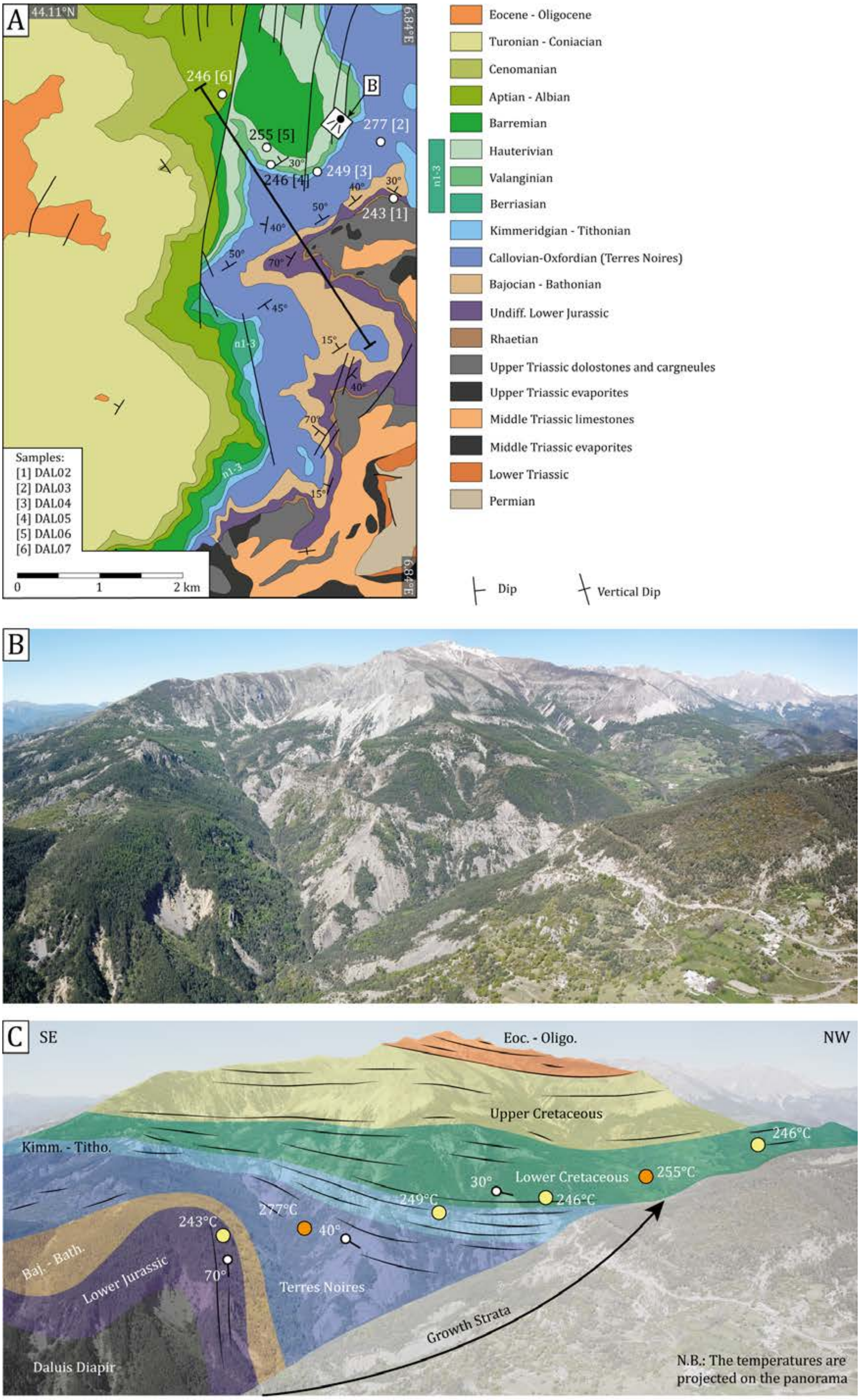

Figure 6 – **A:** Geological map of the Daluis diapir area, modified from the BRGM geological maps at 1/50000 (*Campredon et al.*, 1980). **B:** Uninterpreted and **C:** interpreted panorama of the growth strata flanking the Daluis diapir. See location in A.

4 RSCM Tmax around the Salt Structures: Methodology and Results

4.1 The RSCM Approach

In order to track the potential effect of salt tectonics on Tmax distribution, we have selected 18 carbonaceous material (CM)-rich samples in the Mesozoic sedimentary successions of the area, around several salt-related structures. We use the RSCM approach to calculate Tmax. The RSCM approach is based on the Raman spectra of CM (Figure 7) that changes with increasing temperature (e.g. *Beyssac et al.*, 2002; *Henry et al.*, 2019). Indeed, the maturation of CM is a non-reversible temperature-dependant phenomenon. The organisation of CM evolves with increasing temperature and this organisation affects the resulting Raman spectra. A given spectrum thus reveals a mineral organisation and by extension, a given Tmax achieved by the sample (Figure 7). Among the different existing calibrations through the RSCM literature, we have selected the calibration of *Lahfid et al.* (2010) in order to calculate Tmax between 200 and 350°C and the qualitative analysis of *Saspiturry et al.* (2020) for one sample below 170°C (Table 1). Five samples are in the range 170-190°C which constitutes the lower limit of the *Lahfid et al.* (2010) calibration. For these five samples, we performed both the quantitative calibration of *Lahfid et al.* (2010) and the qualitative analysis of *Saspiturry et al.* (2020). Because the temperatures obtained through both methods are very similar, we present in Table 1 only the values obtained with the quantitative method of *Lahfid et al.* (2010).

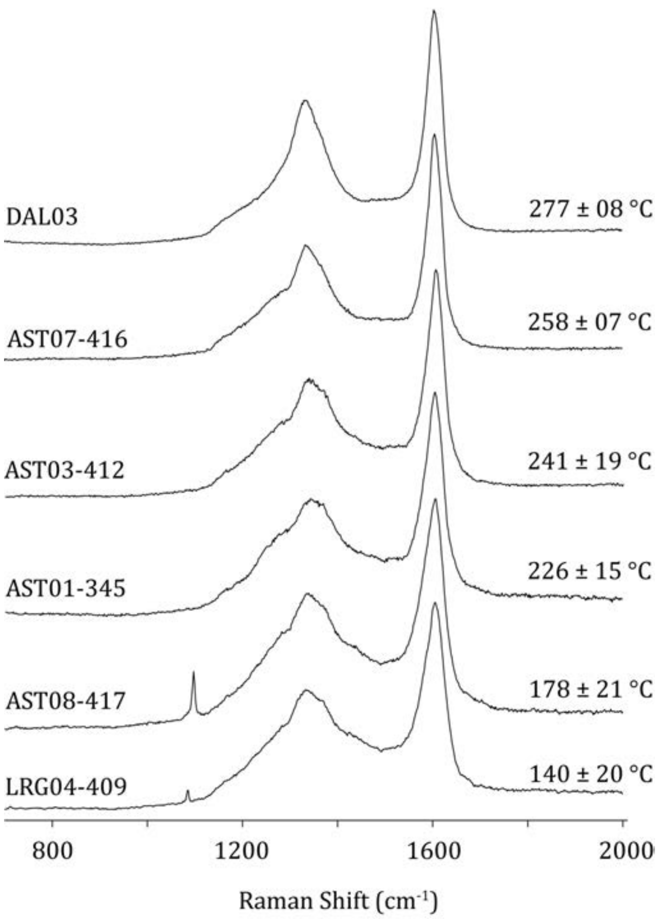

Figure 7 – Representative spectra of carbonaceous material used in this study with the calculated temperature obtained with the *Lahfid et al.* (2010) calibration. Only the LRG04-409 sample temperature has been estimated with the *Saspiturry et al.* (2020) quantitative approach. See details and parameters of the spectra in Table 1.

For this study, the analyses were performed at the Bureau des Recherches Géologiques et Minières (Orléans, France). We used a Renishaw inVia Reflex microspectrometer with a diode-pumped solid-state laser source excitation of 514.5 nm. The laser power that reached the surface of the sample, using a Leica DM2500 microscope and a x100 objective (numerical aperture = 0.90), never exceeded 0.1 mW. The microspectrometer was calibrated with a 520.5 cm^{-1} line of an internal silicon standard for each day of measurement. The Rayleigh diffusion was eliminated by edge filters, and the Raman signal dispersed onto an 1800 lines/mm monochromator before analysis by deep depletion CCD detector (1024 x 256 pixels). When the quality of the samples allowed it, we acquired for each sample 10 to 15 spectra for data consistency.

4.2 Astoin Allochthonous Salt Sheet

Seven samples have been collected in key elements of the structure. Six of these samples are in the Jurassic section beneath the allochthonous salt sheet (Sinemurian, lower Pliensbachian, Bajocian and three in the "Terres Noires" formation, Figure 3A). The last sample is located in the Sinemurian from the "Grande Gautière" which forms the former carapace of the diapiric complex (Figure 3) (*Célini et al.*, 2021). Regarding the samples located beneath the allochthonous salt sheet, the sample in the Sinemurian (AST07-416) of the overturned megaflap shows a temperature of 258 $\pm$ 7°C which is the highest observed around the Astoin diapir. Upsection, the temperatures are 243 $\pm$ 24°C for the Carixian (AST06-415), 242 $\pm$ 11°C for the Bajocian (AST05-414), and 226 $\pm$ 15°C (AST01-345), 241 $\pm$ 19°C (AST03-412) and 227 $\pm$ 16°C (AST04-413) for the three samples from the 'Terres Noires' formation (Figure 3A). The sample from the Sinemurian which formed the diapir carapace shows 178 $\pm$ 21°C (AST08-417, Figure 3A).

4.3 Rocher de Hongrie Megaflap

Five samples have been collected around the Rocher de Hongrie megaflap along a SW-NE section. These samples have been collected as much as possible at a similar elevation (between 500 and 620m) in various stratigraphic units of the Lower and Middle

Table 1 – Samples information and Raman parameters

Sample	Longitude E	Latitude N	Elevation (m)	Lithology	Formation	RA1 mean	Standard deviation RA1	N (spectra)	Temperature (°C)	Standard deviation (°C)
AST01-345	6.146386111	44.33233056	836	Marls	Terres Noires	0.556	0.012	13	226	15
AST03-412	6.162208333	44.34084167	939	Marls	Terres Noires	0.568	0.015	15	241	19
AST04-413	6.169255556	44.34618889	1022	Marls	Terres Noires	0.557	0.013	15	227	16
AST05-414	6.169427778	44.35144722	959	Marly limestone	Bajocian	0.569	0.009	15	242	11
AST06-415	6.169038889	44.3588	1040	Limestone	lower Sinemurian	0.57	0.02	11	243	24
AST07-416	6.165761111	44.36135556	1304	Limestone	Sinemurian	0.582	0.006	15	258	7
AST08-417	6.137858333	44.36783611	1675	Limestone	Sinemurian	0.514	0.018	14	178	21
LRG01-406	5.941505556	44.25655	501	Marls	Terres Noires	37.5	5.6	9	179	29
LRG02-407	5.988411111	44.26690833	573	Marls	Bajocian	35.2	3.1	14	191	20
LRG03-408	6.00175	44.268725	572	Limestone	Lias	35	2	14	192	15
LRG04-409	6.011269444	44.27448889	588	Limestone	Lias			14	140	20
LRG05-410	6.014386111	44.28155556	619	Marls	Terres Noires	35	2.3	15	192	14
DAL02	6.8339	44.07688056	1267	Limestone	Lias	0.57	0.012	15	243	14
DAL03	6.830808333	44.08301389	1341	Marls	Terres Noires	0.597	0.006	15	277	8
DAL04	6.819883333	44.07970556	1361	Limestone	Tithonian	0.575	0.021	15	249	25
DAL05	6.813969444	44.08042222	1365	Marls	Valanginian	0.572	0.015	15	246	18
DAL06	6.813705556	44.08184444	1363	Marly limestone	Hauterivian	0.579	0.009	15	255	11
DAL07	6.804125	44.08911944	1323	Marls	Aptian Albian	0.572	0.01	15	246	11

Jurassic. Three were collected in the SW side of the Rocher de Hongrie in the Terres Noires formation, the Bajocian and the Toarcian. Two were collected in the NE side of the Rocher de Hongrie in the Domerian and the Terres Noires formation. All the samples show Tmax around 180-190°C apart from the sample in the Domerian from the NE side of the salt structure, showing a Tmax of 140 $\pm$ 20°C.

4.4 Daluis Diapir

Six samples have been collected along the Mesozoic section adjoining the Daluis diapir (Figure 6A) to the NW, in the Lower Jurassic, the Terres Noires formation, the Tithonian, the Valanginian, the Hauterivian and the Aptian-Albian. Such as for the Rocher de Hongrie megaflap, the samples have been collected at a relatively similar elevation (between 1260 and 1370m) crosscutting the present-day structure of the Mesozoic strata. All the samples show RSCM Tmax in the range 245 - 255°C apart from the sample collected in the Terres Noires formation which shows a Tmax of 277 $\pm$ 8°C.

5 RSCM Tmax in Salt Tectonics Setting: Interpretation and Discussion

5.1 Astoin Allochthonous Salt Sheet

The obtained RSCM Tmax around the Astoin diapir reveal that the RSCM Tmax progressively decrease upsection and show an anomalously low RSCM Tmax in the Lower Jurassic strata from the carapace (Figure 8B). The Sinemurian in the carapace (Grande Gautière) is about 80°C cooler than the one in the overturned megaflap (Figure 3 and Figure 8), suggesting that the carapace was significantly less warmed during the peak thermal event than the rocks located beneath the advancing allochthonous salt sheet (Figure 8). The development of the Astoin allochthonous salt sheet allowed to the Grande Gautière to be located at shallower depth during the peak thermal event, explaining why it has recorded a cooler temperature than the rocks underneath the salt sheet (Figure 8B). This provide a field example which agrees with the predicted temperature distribution around an allochthonous salt sheet (*Mello et al.*, 1995).

These results fully support the interpretation of the area as a salt-related structured area evidenced by field observations such as progressive overturning and growth strata and abnormal contacts between salt and younger deposits (*Célini et al.*, 2020, 2021). This points out an Early Jurassic initiation of salt activity, and the development of an allochthonous salt sheet from the Middle Jurassic until the Early Cretaceous (Figure 8B) (*Célini et al.*, 2020, 2021). Former interpretations considered the “Grande Gautière” as a klippe of the Digne Nappe (*Arnaud et al.*, 1977; *Gidon*, 1997). But if these units were from the Digne Nappe, the temperatures inside these Lower Jurassic rocks should range between 250°C and 330°C such as in the rocks of similar age belonging to the Digne Nappe (*Célini et al.*, 2023). As it is not the case, the Grande Gautière cannot be regarded as the Digne Nappe remnants but rather as pieces of the carapace of the Astoin diapiric complex, such as proposed by *Célini et al.* (2021). Ignoring salt tectonics involvement in the structuration of the Astoin area could have led to misunderstanding of the temperature distribution. Indeed, by considering the Grande Gautière as a remnant of the Digne Nappe over the Authon-Valavoire thrust sheet, it is difficult to understand the present-day distribution of the RSCM temperatures. A classical purely compressional interpretation with thrusts sheets of

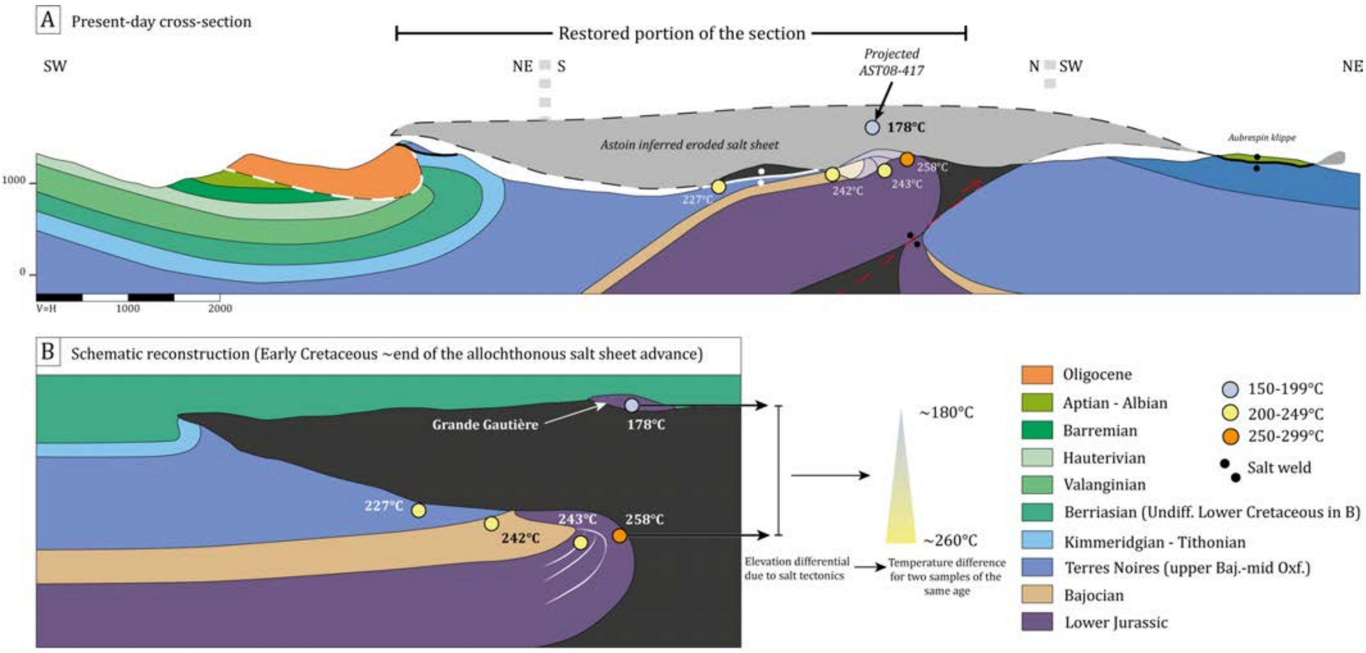

Figure 8 – **A:** Present-day cross-section through the Astoin diapir, modified from *Célini et al.* (2021). **B:** Schematic reconstruction of the Astoin diapir during the Early Cretaceous with the corresponding RSCM temperatures distribution.

the temperatures around the Astoin diapir would have implied a difference of elevation of 2 to 3 km, considering a normal geothermal gradient of 30°C/km, between the Sinemurian samples located in the megaflap and in the carapace (Grande Gautière, Figure 8). Linking the Grande Gautière temperature with the ones in the rest of the Lower Jurassic strata of the Digne Nappe would have implied a very complex structural scenario if one has considered that, because this temperature is much lower, it could mean that the Grande Gautière unit originated from a different structural unit invoking many thrusting phases to explain its present-day position. It appears that, when interpreting the RSCM temperatures in salt-bearing fold-and-thrust belts, one must consider that these temperatures can be influenced by salt tectonics in order to avoid severe misunderstanding of the temperature distribution.

During the RSCM temperature acquisition in Mesozoic times, the geothermal gradient was about 80-90°C/km (*Célini et al.*, 2023). Considering the value 80°C/km, it implies that there was a difference of 1 km of elevation between the sample in the megaflap and the one in the carapace. This means that locally, the allochthonous salt sheet was 1 km thick at least (Figure 8). The geographical extension of such a thick structure during the Mesozoic cannot be considered as minor. The salt sheet might have covered a large area of several tens of square kilometres. Just a few kilometres to the north, the Turriers salt structure also emplaced allochthonous salt during the deposition of the Terres Noires formation (*Célini et al.*, 2020, 2021). In addition, the Astoin diapir is in the NW continuation of the Barles diapir, which also emplaced an allochthonous salt sheet during the Jurassic. Both structures are separated by 10 km. Considering the potential map covering of the Astoin allochtonous salt sheet, it is possible to imagine that the salt sheets from the Astoin, Barles and Turriers diapirs could have joined one each other during the Jurassic, thus forming a salt canopy of regional importance. Other recent studies have highlighted the importance of allochthonous salt sheets in the sub-Alpine chains and the possible occurrence of salt canopies during the Mesozoic (*Brooke-Barnett et al.*, 2023; *Csicsek*, 2023). Such large salt canopies inherited from pre-orogenic stages have also been highlighted in other belts such as the Betics in Spain (e.g. *Pedrera et al.*, 2020; *Flinch and Soto*, 2022), or the Flinders and Willouran Ranges in Australia (e.g. *Hearon et al.*, 2015; *Rowan and Giles*, 2021).

5.2 The Rocher de Hongrie

Regarding the RSCM Tmax at the Rocher de Hongrie, we propose that the formation of the salt structure, occurring during the Lower-Middle Jurassic, pre-dated the thermal event responsible for the observed Tmax, based on the present-day geometry of the Rocher de Hongrie. Samples from the Callovian, Bajocian and Lower Jurassic located on both sides of the salt structure show the same Tmax of ~190°C (Figure 9A). The temperatures distribution around the Rocher de Hongrie highlights two issues. The first one is related to the temperatures that are similar in the Lower Jurassic, Bajocian and Terres Noires formation samples. This suggests that they were located at a similar depth during the Tmax acquisition assuming that there is no lateral heating effect from the salt body. Thus, tracing the isotherm 190°C in a cross-section of the Rocher de Hongrie reveals that it crosscuts the whole structure apart from the NE side of the salt structure where

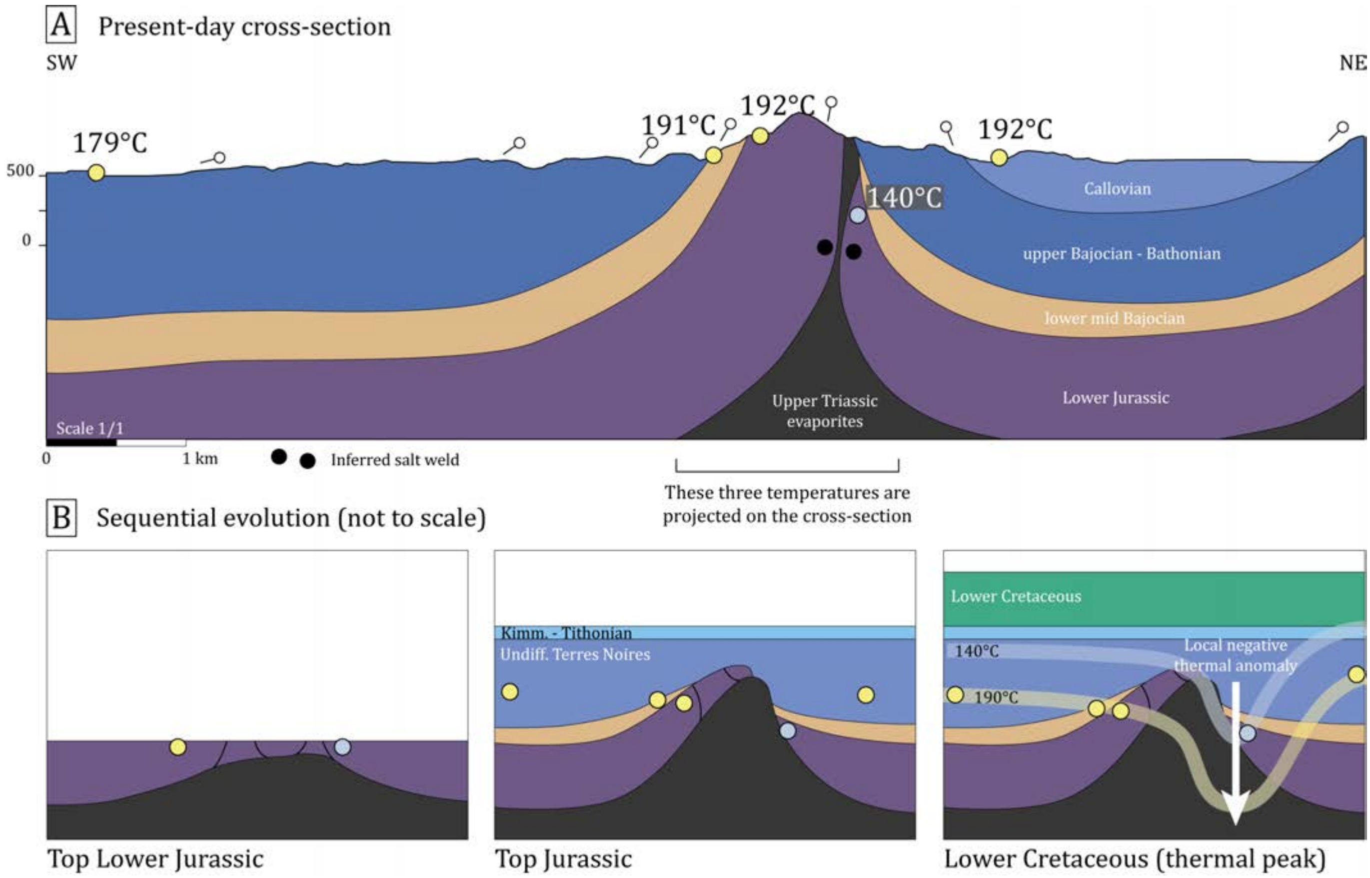

Figure 9 – **A:** Cross-section through the Rocher de Hongrie with the RSCM temperatures anc the corresponding isotherms crossing the structure. The cross-section is the same as in Figure 5. **B:** Schematic evolutionary reconstruction of the Rocher de Hongrie during the Mesozoic.

the Lower Jurassic show a Tmax of 140 ± 20°C (Figure 9A). The second issue regards the fact that the Lower Jurassic sample from the NE side of the Rocher de Hongrie shows a lower Tmax value than the other samples, suggesting that there is a local disorganisation of the isotherms, creating a local negative thermal anomaly located on the NE border of the diapir only and located in the older strata (Figure 9A).

We propose that both issues regarding the temperature distribution are due to salt tectonics. Indeed, considering a normal stacking of undeformed strata or folding, would imply that the older the strata the deeper and thus the hotter, which is not the case here (Figure 9), such as in the Basque-Cantabrian basin (*Ducoux et al.*, 2019) or the Northern Pyrenees (*Izquierdo-Llavall et al.*, 2020). Consequently, the Rocher de Hongrie structure cannot fully be of Alpine age, the strata were deformed prior to the Tmax acquisition due to salt tectonics allowing the samples from the Lower Jurassic, the Bajocian and the Terres Noires formation to be located at a similar elevation during the Tmax acquisition (Figure 9B). This interpretation is also supported by the anomalously low temperature reported in the Lower Jurassic from the NE side of the Rocher de Hongrie. Indeed, a salt structure can function as a thermal dipole dilating the isotherms in its direct neighbouring and creating local negative thermal anomalies toward the base of the salt structure, indicating decreasing temperature (e.g. *Mello et al.*, 1995; *Jensen*, 1983). We propose that the Lower Jurassic sample showing 140 ± 20°C was, at the time of the Tmax acquisition located in the area of the negative anomaly (Figure 9B). *Cedeño et al.* (2019) have shown that the temperatures near the diapir stem can be as much as 70°C lower than expected. Unlike previous models which predict that, apart from the case of an allochthonous salt sheet, symmetrical perturbation of isotherms around salt structures is expected (*Mello et al.*, 1995; *Cedeño et al.*, 2019). Still, it does not explain why this drop of the temperature occurred only in the northern flank of the diapir.

The Rocher de Hongrie diapir shows an asymmetric thermal record around the structure with a negative thermal anomaly in the Lower Jurassic strata in the northern flank of the diapir where the temperature is lower than in the Lower Jurassic from the megaflap (Figure 9). This observation finds an explanation in the variation of salt-related structural style on both sides of the structure (Figure 9), in line with previous studies showing that a non-cylindric salt structure will involve a non-cylindric thermal record (*Grunnaleite and Mosbron*, 2019). Another explanation is to consider the impact of fluid circulations near diapirs (*Canova et al.*, 2018). Diapirism might have favoured the circulation of hot fluids (especially

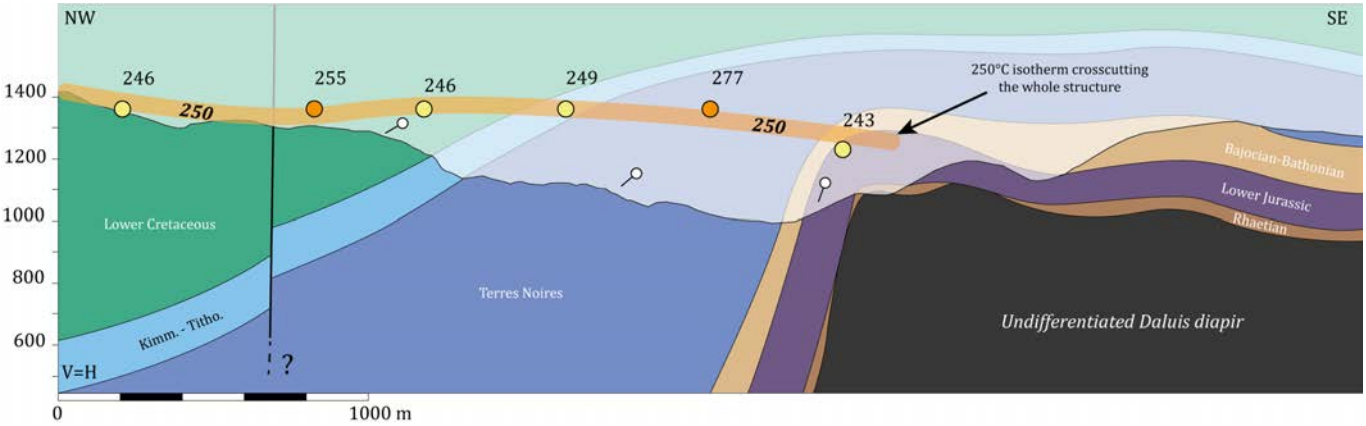

Figure 10 – Present-day cross-section through the Daluis diapir and the associated Mesozoic growth strata. The RSCM temperatures and the 250°C isotherms are reported on the section. See location of the section in Figure 6A)

during the Jurassic-Cretaceous thermal event) in the limestones constituting the megaflap such as in the French Pyrenees (*Motte et al.*, 2021). This assumption is relevant considering previous studies in the Vocontian Domain that have described the contribution of hot fluids circulation during diapirism (*Perthuisot and Guilhaumou*, 1983). The role of fluids would require further geochemical analyses in the megaflap, which are out of the scope of the present study. The anomaly of the Rocher de Hongrie diapir implies that prior to shortening, the salt structure must have been wide enough to allow the deflation of the isotherms on the northern flank (Figure 9B). Thus, it implies that the Rocher de Hongrie diapir has accommodated a substantial amount of shortening by being squeezed during the Cenozoic. Ignoring a potential salt involvement for the formation of the Rocher de Hongrie structure while examining the RSCM temperatures around it, could have led to erroneous interpretation implying a complex structural evolution in order to explain such RSCM temperatures distribution.

5.3 The Daluis Diapir

Except one sample, all the samples located around the Daluis diapir show very close values of RSCM Tmax about 250°C (Figure 6A). In cross-section, the isotherm of 250°C crosscuts the different stratigraphic units and the present-day structure of the Mesozoic strata adjoining the Daluis diapir (Figure 10). The diapiric nature of the structure is known because of field evidence *Dardeau and De Graciansky* (1990); *Brooke-Barnett et al.* (2023) without any contribution of RSCM temperatures. These are the thickness variations testifying for a main diapiric activity during the Jurassic (Figure 6C) and the various abnormal contacts between the evaporites and cargneules with younger strata of the Jurassic (Figure 6A). The Daluis diapir developed since the Early Jurassic until at least the end of the Late Cretaceous (*Dardeau and De Graciansky*, 1990; *Brooke-Barnett et al.*, 2023). The peak thermal event affecting the SW Alps during the Early Cretaceous has overprinted an already existing structure as shown by the isotherms crossing all the stratigraphic units in its NW limb (Figure 10). The Daluis diapir constitutes another example where the thermal imprint responsible for the calculated RSCM Tmax occurred after the salt-related deformation of post-salt strata, allowing the isotherms to overprint an existing structure. This is similar to what has been observed in the northern Pyrenees where salt-related deformation occurred prior to the acquisition of the main thermal event during the Cretaceous, as revealed by the pattern of isotherms overprinting the whole structure of the "Chaînons Béarnais" (*Izquierdo-Llavall et al.*, 2020) or those of the Nappe des Marbres in the Basco-Cantabrian belt (*Ducoux et al.*, 2019).

At Daluis, the thermal record can be reproduced by a late thermal imprint during the Alpine orogeny involving at least 8 km of syn-orogenic deposits and/or tectonic nappes above. However, this hypothesis conflicts with petrologic and thermochronology data showing that around Daluis, the Eocene-Oligocene syn-orogenic deposits have been buried to depths of 4-6 km (*Labaume et al.*, 2008). Thus, we infer that the thermal peak occurred prior to the Alpine orogeny, i.e., during the Jurassic-Early Cretaceous extensional events (*Célini et al.*, 2023). At that time, ignoring salt tectonics would not allow to understand why the isotherm 250°C crosscuts the structure. The Daluis diapir therefore constitutes an example for which salt tectonics along with inherited thermal events must be considered in order to explain temperature distribution around the structure. Ignoring the thermal effects of these processes can lead to an overestimation of the thickness of syn-orogenic deposits or nappe stack, which in turns possibly leads to an overestimation of the calculated shortening.

5.4 Regional scale variations in the thermal peak record

The thermal peak recorded at the Rocher de Hongrie is 60-70°C lower than at Daluis and Astoin. We find an explanation to this in the distribution of the three salt structures that are in various structural units (Figure 1). The Rocher de Hongrie is n the autochthonous while the Daluis and Astoin structures are respectively located in the Digne and Authon-Valavoire thrust sheets, which have been transported from their initial to present-day locations over several kilometres towards the SW (e.g. *Gidon and Pairis*, 1992; *Gidon*, 1997; *Célini et al.*, 2020). During, the Early Cretaceous, they were located nearer to the Valaisan Domain thus in an area where the lithosphere was extremely thin (*Célini et al.*, 2023). Thus, they might have recorded a higher thermal event than the Rocher de Hongrie.

6 Conclusions

We performed the RSCM approach on a series of samples located around identified salt structures of the SW sub-Alpine fold-and-thrust belt. Our results highlight that the structures were already deformed by Jurassic salt tectonics when the RSCM temperatures were acquired during the peak thermal event of the Early Cretaceous. At Astoin, salt tectonics has allowed for samples of the same age to acquire very distinct RSCM temperatures, highlighting how salt tectonics can influence temperature distribution. Astoin and the Rocher de Hongrie both testify for the fact that, in a syn-compressional Alpine scenario, the interpretation of the RSCM temperatures would have been very difficult without considering salt tectonics. It is primordial to apprehend all the possible structural evolutions of a structure when examining the RSCM temperatures distribution around it, and especially to consider that if salt is present, it can influence this distribution at the local scale. Conversely, the RSCM temperatures allowed to identify that the Rocher de Hongrie must have accommodated an important part of the Alpine shortening and that the allochthonous salt sheet of Astoin was of regional importance.

Acknowledgements

Authors are grateful to the two reviewers and Associate Editor Berta Lopez-Mir for their thorough comments on the manuscript. Authors are also grateful to the Executive Editor Gwenn Peron-Pinvidic and the Technical Editor Mohamed Gouiza for their handling of the manuscript.

Author contributions

Conceptualisation: NC, JPC, AL, FM. Analysis: NC, AL. Field work: NC, JPC, AL, FM. Writing - original draft: NC Writing - review and editing: NC, JPC, AL, FM. Funding Acquisition: JPC, AL, FM.

Data availability

All the data used in this article are available upon request.

Competing interests

The authors declare no competing interests.

Peer review

This publication was peer-reviewed by Laura Burrel and Esther Izquierdo Lavall. The full peer-review report can be found here: tektonika.online/index.php/home/article/view/60/77

Copyright notice

References

Alsop, G. I., R. Weinberger, S. Marco, and T. Levi (2018), Fault and fracture patterns around a strike-slip influenced salt wall, *Journal of Structural Geology*, *106*, 103–124, doi: 10.1016/j.jsg.2017.10.010.

Angiboust, S., R. Langdon, P. Agard, D. Waters, and C. Chopin (2012), Eclogitization of the monviso ophiolite (w. alps) and implications on subduction dynamics, *Journal of Metamorphic Geology*, *30*(1), 37–61, doi: 10.1111/j.1525-1314.2011.00951.x.

Angiboust, S., J. Glodny, O. Oncken, and C. Chopin (2014), In search of transient subduction interfaces in the dent Blanche–Sesia tectonic system (w. alps), *Lithos*, *205*, 298–321, doi: 10.1016/j.lithos.2014.07.001.

Angrand, P., and F. Mouthereau (2021), Evolution of the alpine orogenic belts in the western mediterranean region as resolved by the kinematics of the Europe-Africa diffuse plate boundary, *BSGF - Earth Sciences Bulletin*, *192*, doi: 10.1051/bsgf/2021031.

Apps, G., F. Peel, and T. Elliott (2004), The structural setting and palaeogeographical evolution of the grès d'annot basin, *Geological Society, London, Special Publications*, *221*(1), 65–96, doi: 10.1144/GSL.SP.2004.221.01.05.

Arlhac, P., and C. Rousset (1979), La nappe de digne près de gap (Hautes-Alpes) : sa place dans les alpes externes françaises, *Comptes Rendus de l'Académie des Sciences de Paris*, *288*(D), 47–50.

Arlhac, P., B. Beaudoin, C. Kerckhove, J. Rouire, and C. Rousset (1983), Carte géologique de la france à 1/50000, feuille 894, seyne.

Arnaud, H., M. Gidon, and J.-L. Pairis (1977), Précisions sur la structure des chaînes subalpines méridionales dans la région de Faucon-Turriers-Clamensane (alpes de Haute-Provence), *Géologie alpine*, *53*, 5–34.

Artru, P. (1967), Le contrôle structural de la sédimentation argileuse dans les terres noires jurassiques, d'embrun à la vallée du rhône (france), *Bulletin du Service de la carte géologique d'Alsace et de Lorraine*, *20*(4), 211–222, doi: 10.3406/sgeol.1967.1323.

Artru, P. (1972), Les terres noires du bassin rhodanien (bajocien supérieur à oxfordien moyen): stratigraphie, sédimentologie, géochimie-alpes françaises, Ph.D. thesis, Université Claude Bernard-Lyon I.

Balansa, J., A. Lahfid, N. Espurt, J.-C. Hippolyte, P. Henry, S. Caritg, and B. Fasentieux (2023), Unraveling the eroded units of mountain belts using RSCM thermometry and cross-section balancing: example of the southwestern french alps, *Geologische Rundschau: Zeitschrift fur allgemeine Geologie*, *112*(2), 443–458, doi: 10.1007/s00531-022-02257-3.

Baudrimont, F., and P. Dubois (1977), Un bassin mésogéen du domaine péri-alpin : le sud-est de la france, *Bulletin Centres Rech. Explor. -Prod. Elf-Aquitaine*, *1*(1), 261–308.

Bellanger, M., R. Augier, N. Bellahsen, L. Jolivet, P. Monié, T. Baudin, and O. Beyssac (2015), Shortening of the european dauphinois margin (oisans massif, western alps): New insights from RSCM maximum temperature estimates and 40Ar/39Ar in situ dating, *Journal of Geodynamics*, *83*, 37–64, doi: 10.1016/j.jog.2014.09.004.

Beltrando, M., D. Rubatto, R. Compagnoni, and G. Lister (2007), Was the valaisan basin floored by oceanic crust? evidence of permian intra-plate magmatism in the versoyen unit (valaisan domain, NW alps), *Ofioliti*, *32*(2), 15, doi: 10.7892/boris.85691.

Berástegui, X., C. J. Banks, C. Puig, C. Taberner, D. Waltham, and M. Fernàndez (1998), Lateral diapiric emplacement of triassic evaporites at the southern margin of the guadalquivir basin, spain, *Geological Society, London, Special Publications*, *134*(1), 49–68, doi: 10.1144/GSL.SP.1998.134.01.04.

Bestani, L., N. Espurt, J. Lamarche, O. Bellier, and F. Hollender (2016), Reconstruction of the provence chain evolution, southeastern france, *Tectonics*, *35*(6), 1506–1525, doi: 10.1002/2016tc004115.

Beucher, R., P. van der Beek, J. Braun, and G. E. Batt (2012), Exhumation and relief development in the pelvoux and Dora-Maira massifs (western alps) assessed by spectral analysis and inversion of thermochronological age transects, *Journal of geophysical research*, *117*(F3), 1–22, doi: 10.1029/2011jf002240.

Beyssac, O., B. Goffé, C. Chopin, and J. N. Rouzaud (2002), Raman spectra of carbonaceous material in metasediments: a new geothermometer, *Journal of Metamorphic Geology*, *20*(9), 859–871, doi: 10.1046/j.1525-1314.2002.00408.x.

Bigot-Cormier, F., M. Sosson, G. Poupeau, J.-F. Stéphan, and E. Labrin (2006), The denudation history of the argentera alpine external crystalline massif (western alps, France-Italy): an overview from the analysis of fission tracks in apatites and zircons, *Geodinamica Acta*, *19*(6), 455–473, doi: 10.3166/ga.19.455-473.

Bonini, M. (2003), Detachment folding, fold amplification, and diapirism in thrust wedge experiments, *Tectonics*, *22*(6), doi: 10.1029/2002tc001458.

Boutoux, A., N. Bellahsen, U. Nanni, R. Pik, A. Verlaguet, Y. Rolland, and O. Lacombe (2016), Thermal and structural evolution of the external western alps: Insights from (U–Th–Sm)/He thermochronology and RSCM thermometry in the aiguilles Rouges/Mont blanc massifs, *Tectonophysics*, *683*, 109–123, doi: 10.1016/j.tecto.2016.06.010.

Brooke-Barnett, S., R. Graham, L. Lonergan, and L. A. Csicsek (2023), Salt tectonics along a strike-slip fault system in the sub-alpine chains of southeastern france, from the triassic to the oligocene, *AAPG bulletin*, *107*(1), 87–122, doi: 10.1306/08042221102.

Brun, J.-P., and X. Fort (2004), Compressional salt tectonics (angolan margin), *Tectonophysics*, *382*(3), 129–150, doi: 10.1016/j.tecto.2003.11.014.

Burrel, L., and A. Teixell (2021), Contractional salt tectonics and role of pre-existing diapiric structures in the southern pyrenean foreland fold–thrust belt (montsec and serres marginals), *Journal of the Geological Society*, *178*(4), jgs2020–085, doi: 10.1144/jgs2020-085.

Callot, J.-P., S. Jahani, and J. Letouzey (2007), The role of pre-existing diapirs in fold and thrust belt development, in *Thrust Belts and Foreland Basins*, edited by O. Lacombe, J. Lavé, F. Roure, and J. Vergés, pp. 309–325, Springer-Verlag Berlin Heidelberg.

Callot, J.-P., V. Trocmé, J. Letouzey, E. Albouy, S. Jahani, and S. Sherkati (2012), Pre-existing salt structures and the folding of the zagros mountains, *Geological Society, London, Special Publications*, *363*(1), 545–561, doi: 10.1144/SP363.27.

Cámara, P. (2017), Chapter 17 - salt and Strike-Slip tectonics as main drivers in the structural evolution of the Basque-Cantabrian basin, spain, in *Permo-Triassic Salt Provinces of Europe, North Africa and the Atlantic Margins*, edited by J. I. Soto, J. F. Flinch, and G. Tari, pp. 371–393, Elsevier, doi: 10.1016/B978-0-12-809417-4.00018-5.

Campredon, R., P. Aicard, A. Bambier, and G. Durozoy (1980), Notice explicatiove, carte géol. france (1/50000), feuille ENTREVAUX (945), *Tech. rep.*, BRGM.

Canérot, J., M. R. Hudec, and K. Rockenbauch (2005), Mesozoic diapirism in the pyrenean orogen: Salt tectonics on a transform plate boundary, *AAPG bulletin*, *89*(2), 211–229, doi: 10.1306/09170404007.

Canova, D. P., M. P. Fischer, R. S. Jayne, and R. M. Pollyea (2018), Advective heat transport and the salt chimney effect: A numerical analysis, *Geofluids*, *2018*, 18, doi: 10.1155/2018/2378710.

Carrapa, B., J. Wijbrans, and G. Bertotti (2003), Episodic exhumation in the Western Alps, *Geology*, *31*(7), 601–604, doi: 10.1130/0091-7613(2003)031<0601:EEITWA>2.0.CO;2.

Cedeño, A., L. A. Rojo, N. Cardozo, L. Centeno, and A. Escalona (2019), The impact of salt tectonics on the thermal evolution and the petroleum system of confined rift basins: Insights from basin modeling of the nordkapp basin, norwegian barents sea, *Geosciences Journal*, *9*(7), 316, doi: 10.3390/geosciences9070316.

Célini, N. (2020), Le rôle des évaporites dans l'évolution tectonique du front alpin : cas de la nappe de digne, Ph.D. thesis, Université de Pau et des Pays de l'Adour.

Célini, N., J. Callot, J. Ringenbach, and R. Graham (2020), Jurassic salt tectonics in the SW sub-alpine fold-and-thrust belt, *Tectonics*, *39*(10), e2020TC006,107, doi: 10.1029/2020tc006107.

Célini, N., J.-P. Callot, J.-C. Ringenbach, and R. Graham (2021), Anatomy and evolution of the astoin diapiric complex, sub-alpine fold-and-thrust belt (france), *Bulletin de la Societe Geologique de France*, *192*, 29, doi: 10.1051/bsgf/2021018.

Célini, N., J.-P. Callot, A. Pichat, E. Legeay, R. Graham, and J.-C. Ringenbach (2022), Secondary minibasins in orogens: Examples from the sivas basin (turkey) and the sub-alpine fold-and-thrust belt (france), *Journal of Structural Geology*, *156*, 104,555, doi: 10.1016/j.jsg.2022.104555.

Célini, N., F. Mouthereau, A. Lahfid, C. Gout, and J.-P. Callot (2023), Rift thermal inheritance in the SW alps (france): insights from RSCM thermometry and 1D thermal numerical modelling, *Solid earth*, *14*(1), 1–16, doi: 10.5194/se-14-1-2023.

Chantraine, J., A. Autran, C. Cavelier, B. Alabouvette, J. C. Barféty, F. Cecca, L. Clozier, S. Debrand-Passard, J. Dubreuilh, J. L. Feybesse, and Others (1996), Carte géologique de la france à 1/1 000 000.

Costa, E., and B. C. Vendeville (2002), Experimental insights on the geometry and kinematics of fold-and-thrust belts above weak, viscous evaporitic décollement, *Journal of Structural Geology*, *24*(11), 1729–1739, doi: 10.1016/S0191-8141(01)00169-9.

Cotton, J. T., and H. A. Koyi (2000), Modeling of thrust fronts above ductile and frictional detachments: Application to structures in the salt range and potwar plateau, pakistan, *GSA Bulletin*, *112*(3), 351–363, doi: 10.1130/0016-7606(2000)112<351:MOTFAD>2.0.CO;2.

Coward, M., and D. Dietrich (1989), Alpine tectonics — an overview, *Geological Society, London, Special Publications*, *45*(1), 1–29, doi: 10.1144/GSL.SP.1989.045.01.01.

Crémades, A., M. Ford, and J. Charreau (2021), Evidence of decoupled deformation during jurassic rifting and cenozoic inversion phases in the salt-rich Corbières-Languedoc transfer zone (Pyreneo-Provencal orogen, france), *Bulletin de la Société Géologique de France*, *192*(1), 37, doi: 10.1051/bsgf/2021022.

Crumeyrolle, P., J.-L. Rubino, and G. Clauzon (1991), Miocene depositional sequences within a tectonically controlled transgressive-regressive cycle, in *Sedimentation, Tectonics and Eustasy: Sea-Level Changes at Active Margins*, edited by D. I. M. MacDonald, pp. 373–390, Blackwell Scientific.

Csicsek, L. A. (2023), The influence of salt tectonics in the evolution of the subalpine chains, Haute-Provence, france, Ph.D. thesis, Imperial College London.

Cumberpatch, Z. A., I. A. Kane, E. L. Soutter, D. M. Hodgson, C. A.-L. Jackson, B. A. Kilhams, and Y. Poprawski (2021), Interactions between deep-water gravity flows and active salt tectonics, *Journal of Sedimentary Research*, *91*(1), 34–65, doi: 10.2110/jsr.2020.047.

Curnelle, R., and P. Dubois (1986), Evolution mesozoique des grands bassins sedimentaires francais; bassins de paris, d'aquitaine et du Sud-Est, *Bulletin de la Societe Geologique de France*, *II*(4), 529–546, doi: 10.2113/gssgfbull.ii.4.529.

Dardeau, G., and P. C. De Graciansky (1990), Halocinèse et rifting téthysien dans les Alpes-Maritimes (france), *Bulletin des centres de recherches exploration-Production Elf-Aquitaine*, *14*(2), 443–464.

Dardeau, G., D. Fortwengler, d. P.-C. Graciansky, T. Jacquin, D. Marchand, and J. Martinod (1990), Halocinèse et jeu de blocs dans les baronnies : diapirs de propiac, montaulieu, condorcet (département de la drôme, france), *Bulletin Centres Rech. Explor. -Prod. Elf-Aquitaine*, *14*, 111–151.

Davis, D. M., and T. Engelder (1985), The role of salt in fold-and-thrust belts, *Tectonophysics*, *119*(1-4), 67–88, doi: 10.1016/0040-1951(85)90033-2.

Davison, I., and T. A. Cunha (2017), Allochthonous salt sheet growth: Thermal implications for source rock maturation in the deepwater burgos basin and perdido fold belt, mexico, *Interpretation*, *5*(1), T11–T21, doi: 10.1190/int-2016-0035.1.

de Graciansky, P. C., and M. Lemoine (1988), Early Cretaceous extensional tectonics in the southwestern French Alps; a consequence of North-Atlantic rifting during Tethyan spreading, *Bulletin de la Société Géologique de France*, *IV*(5), 733–737, doi: 10.2113/gssgfbull.IV.5.733.

de Graciansky, P. C., G. Dardeau, M. Lemoine, and P. Tricart (1989), The inverted margin of the french alps and foreland basin inversion, *Geological Society, London, Special Publications*, *44*(1), 87–104, doi: 10.1144/GSL.SP.1989.044.01.06.

de Graciansky, P.-C., D. G. Roberts, and P. Tricart (2010), *The Western Alps, from Rift to Passive Margin to Orogenic Belt: An Integrated Geoscience Overview*, Elsevier.

Debrand-Passard, S., S. Courbouleix, and M.-J. Lienhardt (1984), *Synthèse géologique du Sud-Est de la France, Mém. BRGM FR*, BRGM.

Decarlis, A., M. G. Fellin, M. Maino, S. Ferrando, G. Manatschal, L. Gaggero, S. Seno, F. M. Stuart, and M. Beltrando (2017), Tectono-thermal evolution of a distal rifted margin: Constraints from the calizzano massif (Prepiedmont-Brianconnais domain, ligurian alps), *Tectonics*, *36*(12), 3209–3228, doi: 10.1002/2017TC004634.

Decrausaz, T., O. Müntener, P. Manzotti, R. Lafay, and C. Spandler (2021), Fossil oceanic core complexes in the alps. new field, geochemical and isotopic constraints from the tethyan aiguilles rouges ophiolite (val d'hérens, western alps, switzerland), *Swiss Journal of Geosciences*, *114*(1), 3, doi: 10.1186/s00015-020-00380-4.

Deville, E., and W. Sassi (2006), Contrasting thermal evolution of thrust systems: An analytical and modeling approach in the front of the western alps, *AAPG bulletin*, *90*(6), 887–907, doi: 10.1306/01090605046.

Di Vincenzo, G., S. Tonarini, B. Lombardo, D. Castelli, and L. Ottolini (2006), Comparison of 40Ar–39Ar and Rb–Sr data on phengites from the UHP Brossasco–Isasca unit (dora maira massif, italy): Implications for dating white mica, *Journal of Petrology*, *47*(7), 1439–1465, doi: 10.1093/petrology/egl018.

Dooley, T., K. R. McClay, M. Hempton, and D. Smit (2005), Salt tectonics above complex basement extensional fault systems: results from analogue modelling, in *Petroleum Geology: North-West Europe and Global Perspectives—Proceedings of the 6th Petroleum Geology Conference*, vol. 6, edited by A. G. Doré and B. A. Vining, p. 0, Geological Society of London, doi: 10.1144/0061631.

Ducoux, M., L. Jolivet, J.-P. Callot, C. Aubourg, E. Masini, A. Lahfid, E. Homonnay, F. Cagnard, C. Gumiaux, and T. Baudin (2019), The nappe des marbres unit of the basque-cantabrian basin: The tectono-thermal evolution of a fossil hyperextended rift basin, *Tectonics*, *38*(11), 3881–3915, doi: 10.1029/2018tc005348.

Duffy, O. B., T. P. Dooley, M. R. Hudec, M. P. A. Jackson, N. Fernandez, C. A.-L. Jackson, and J. I. Soto (2018), Structural evolution of salt-influenced fold-and-thrust belts: A synthesis and new insights from basins containing isolated salt diapirs, *Journal of Structural Geology*, *114*, 206–221, doi: 10.1016/j.jsg.2018.06.024.

Dumont, T. (1984), Le rhétien et le lias inférieur prépiémontais: enregistrement sédimentaire du passage des carbonates de plate-forme triasiques au jurassique hémipélagique lors du début du rifting téthysien, *Géologie Alpine*, *60*, 13–25.

Dumont, T. (1988), Late triassic - early jurassic evolution of the western alps and of their european foreland ; initiation of the tethyan rifting, *Bulletin de la Société Géologique de France*, *IV*(4), 601–611.

Dumont, T., T. Simon-Labric, C. Authemayou, and T. Heymes (2011), Lateral termination of the north-directed alpine orogeny and onset of westward escape in the western alpine arc: Structural and sedimentary evidence from the external zone, *Tectonics*, *30*(5), 1–31, doi: 10.1029/2010tc002836.

Dumont, T., S. Schwartz, S. Guillot, T. Simon-Labric, P. Tricart, and S. Jourdan (2012), Structural and sedimentary records of the oligocene revolution in the western alpine arc, *Journal of Geodynamics*, *56-57*, 18–38, doi: 10.1016/j.jog.2011.11.006.

Emre, T. (1977), Contribution à l'étude de quelques diapirs du SE de la france, Ph.D. thesis, Université Scientifique et Médicale de Grenoble.

Emre, T., and G. Truc (1978), Mise en évidence d'un contact discordant Oligocène-Trias dans le massif de suzette . implications tectoniques et conséquences sur l'origine des évaporites ludiennes du bassin de mormoiron (vaucluse), *Géologie Alpine*, *54*, 17–23.

Espurt, N., F. Wattellier, J. Philip, J.-C. Hippolyte, O. Bellier, and L. Bestani (2019), Mesozoic halokinesis and basement inheritance in the eastern provence fold-thrust belt, SE france, *Tectonophysics*, *766*, 60–80, doi: 10.1016/j.tecto.2019.04.027.

Faucher, T., M. Gidon, J.-L. Pairis, and G. Mascle (1988), Directions de transport au front de la nappe de digne (chaînes subalpines méridionales), *Comptes Rendus de l'Académie des Sciences de Paris*, *306*(II), 227–230.

Fernandez, N., and B. J. P. Kaus (2014), Influence of pre-existing salt diapirs on 3D folding patterns, *Tectonophysics*, *637*, 354–369, doi: 10.1016/j.tecto.2014.10.021.

Flinch, J. F., and J. I. Soto (2017), Chapter 19 - allochthonous triassic and salt tectonic processes in the Betic-Rif orogenic arc, in *Permo-Triassic Salt Provinces of Europe, North Africa and the Atlantic Margins*, edited by J. I. Soto, J. F. Flinch, and G. Tari, pp. 417–446, Elsevier, doi: 10.1016/B978-0-12-809417-4.00020-3.

Flinch, J. F., and J. I. Soto (2022), Structure and alpine tectonic evolution of a salt canopy in the western betic cordillera (spain), *Marine and Petroleum Geology*, *143*(105782), 105,782, doi: 10.1016/j.marpetgeo.2022.105782.

Flinch, J. F., A. W. Bally, and S. Wu (1996), Emplacement of a passive-margin evaporitic allochthon in the betic cordillera of spain, *Geology*, *24*(1), 67–70, doi: 10.1130/0091-7613(1996)024<0067:EOAPME>2.3.CO;2.

Ford, Lickorish, and Kusznir (1999), Tertiary foreland sedimentation in the southern subalpine chains, SE france: a geodynamic appraisal, *Basin Research*, *11*(4), 315–336, doi: 10.1046/j.1365-2117.1999.00103.x.

Ford, M., and W. H. Lickorish (2004), Foreland basin evolution around the western alpine arc, *Geological Society, London, Special Publications*, *221*(1), 39–63, doi: 10.1144/GSL.SP.2004.221.01.04.

Ford, M., and J. Vergés (2020), Evolution of a salt-rich transtensional rifted margin, eastern north pyrenees, france, https://www.lyellcollection.org/doi/10.1144/jgs2019-157, doi: 10.1144/jgs2019-157, accessed: 2024-2-12.

Ford, M., S. Duchene, D. Gasquet, and O. Vanderhaeghe (2006), Two-phase orogenic convergence in the external and internal SW alps, https://www.lyellcollection.org/doi/10.1144/0016-76492005-034, doi: 10.1144/0016-76492005-034, accessed: 2024-2-12.

Fornel, E. D., P. Joseph, G. Désaubliaux, R. Eschard, F. Guillocheau, O. Lerat, C. Muller, C. Ravenne, and K. Sztrákos (2004), The southern grès d'annot outcrops (french alps): an attempt at regional correlation, *Geological Society special publication*, *221*, 137–160, doi: 10.1144/GSL.SP.2004.221.01.08.

Fry, N. (1989), Southwestward thrusting and tectonics of the western alps, https://www.lyellcollection.org/doi/10.1144/GSL.SP.1989.045.01.05, doi: 10.1144/GSL.SP.1989.045.01.05, accessed: 2024-2-12.

Gabalda, S., O. Beyssac, L. Jolivet, P. Agard, and C. Chopin (2009), Thermal structure of a fossil subduction wedge in the western alps, *Terra nova*, *21*(1), 28–34, doi: 10.1111/j.1365-3121.2008.00849.x.

Gannaway Dalton, C. E., K. A. Giles, J. A. Muñoz, and M. G. Rowan (2022), Interpreting the nature of the aulet and adons diapirs from sedimentologic and stratigraphic analysis of flanking minibasin strata, spanish pyrenees, catalunya, spain, *Journal of Sedimentary Research*, *92*(3), 167–209, doi: 10.2110/jsr.2021.179.

Gebauer, D., H.-P. Schertl, M. Brix, and W. Schreyer (1997), 35 ma old ultrahigh-pressure metamorphism and evidence for very rapid exhumation in the dora maira massif, western alps, *Lithos*, *41*(1), 5–24, doi: 10.1016/S0024-4937(97)82002-6.

Gidon, M. (1971), Notice explicative, carte géologique de la france à 1/50000, feuille 869, gap, *Tech. rep.*, BRGM.

Gidon, M. (1979), Le rôle des étapes successives de déformation dans la tectonique alpine du massif du pelvoux (alpes occidentales), *C. R. Acad. Sc. Paris*, *288*(D), 803–806.

Gidon, M. (1997), Les chaînons subalpins au nord-est de sisteron et l'histoire tectonique de la nappe de digne, *Géologie Alpine*, *73*, 23–57.

Gidon, M., and J.-L. Pairis (1986a), La nappe de digne (chaînes subalpines méridionales) : origine, déplacement et signification régionale, *Comptes Rendus de l'Académie des Sciences de Paris*, *3030*(II), 981–984, doi: 0249-6305/86/03030981.

Gidon, M., and J.-L. Pairis (1986b), Problèmes d'autochtonie et de charriage aux confins méridionaux du dôme de remollon (environs de turriers, Alpes-de-Haute-Provence), *Géologie de la France*, *4*, 417–432.

Gidon, M., and J.-L. Pairis (1992), Relations entre le charriage de la nappe de digne et la structure de sonautochtone dans la vallée du bès (alpes de Haute-Provence, france), *Eclogae Geologicae Helvetiae*, *85*(2), 327–359.

Gidon, M., M. Moullade, G. Montjuvent, and J. Flandrin (1991a), Carte géologique de la france à 1/50000, feuille 893, Laragne-Montéglin.

Gidon, M., G. Montjuvent, J. Flandrin, M. Moullade, G. Durozoy, and L. Damiani (1991b), Notice explicative, carte géologique de la france (1/50000), feuille Laragne-Montéglin (893) - orléans : BRGM, *Tech. rep.*, BRGM.

Gigot, P., and D. Haccard (1970), A propos de l'âge anté-éocène supérieur d'une struture diapirique située près de Saint-Geniez (Alpes-de-Haute-Provence) et de ses conséquences structurales, *Compte Rendu Sommaire de l Société Géologique de France*, pp. 319–321.

Gigot, P., P. Cotillon, D. Haccard, G. Montjuvent, and G. Dardeau (2013), Carte géologique de la france à 1/50000, feuille 917, sisteron.

Giles, K. A., and T. F. Lawton (1999), Attributes and evolution of an exhumed salt weld, la popa basin, northeastern mexico, *Geology*, *27*(4), 323–326, doi: 10.1130/0091-7613(1999)027<0323:AAEOAE>2.3.CO;2.

Giles, K. A., and T. F. Lawton (2002), Halokinetic sequence stratigraphy adjacent to the el papalote diapir, northeastern mexico, *AAPG bulletin*, *86*(5), 823–840, doi: 10.1306/61eedbac-173e-11d7-8645000102c1865d.

Giles, K. A., and M. G. Rowan (2012), Concepts in halokinetic-sequence deformation and stratigraphy, *Geological Society, London, Special Publications*, *363*(1), 7–31, doi: 10.1144/SP363.2.

Girault, J. B., N. Bellahsen, A. Boutoux, C. L. Rosenberg, U. Nanni, A. Verlaguet, and O. Beyssac (2020), The 3-d thermal structure of the helvetic nappes of the european alps: Implications for collisional processes, *Tectonics*, *39*(3), e2018TC005,334, doi: 10.1029/2018tc005334.

Girault, J. B., N. Bellahsen, M. Bernet, R. Pik, N. Loget, E. Lasseur, C. L. Rosenberg, M. Balvay, and M. Sonnet (2022), Exhumation of the western alpine collisional wedge: New thermochronological data, *Tectonophysics*, *822*(March 2021), 229,155, doi: 10.1016/j.tecto.2021.229155.

Glotzbach, C., J. Reinecker, M. Danišik, M. Rahn, W. Frisch, and C. Spiegel (2008), Neogene exhumation history of the mont blanc massif, western alps, *Tectonics*, *27*(4), doi: 10.1029/2008TC002257.

Glotzbach, C., P. A. van der Beek, and C. Spiegel (2011), Episodic exhumation and relief growth in the mont blanc massif, western alps from numerical modelling of thermochronology data, *Earth and planetary science letters*, *304*(3), 417–430, doi: 10.1016/j.epsl.2011.02.020.

Goguel, J. (1939), Tectonique des chaînes subalpines entre la bléone et la durance- alpes, *Bulletin des Services de la Carte Géologique de France*, *202*(XLI), 1–48.

Graciansky, d. P.-C., J.-L. Rudkiewicz, and P. Samec (1986), Tectonique salifère d'âge jurassique dans la zone subbriançonnaise (alpes de savoie, france) : rôle dans le découpage en nappes de charriage et leur progression, *Comptes Rendus de l'Académie des Sciences de Paris*, *302*(II), 891–896.

Graham, R., and A. Csicsek (2020), The barreme basin and the gevaudan diapir - an example of the interplay between compressional tectonics and salt diapirism, in *EGU General Assembly 2020*, EGU2020-3655, Copernicus Meetings, doi: 10.5194/egusphere-egu2020-3655.

Graham, R., M. Jackson, R. Pilcher, and B. Kilsdonk (2012), Allochthonous salt in the sub-alpine fold–thrust belt of haute provence, france, *Geological Society, London, Special Publications*, *363*(1), 595–615, doi: 10.1144/SP363.30.

Graham, R. H., S. Brooke-barnett, L. A. Csicsek, L. Lonergan, N. Célini, J.-P. Callot, and J.-C. Ringenbach (2019), Allochthonous salt in the fold and thrust belt of haute provence, S.W.Alps, in *81st EAGE Conference and Exhibition 2019*, doi: 10.3997/2214-4609.201901289.

Granado, P., E. Roca, P. Strauss, K. Pelz, and J. A. Muñoz (2019), Structural styles in fold-and-thrust belts involving early salt structures: The northern calcareous alps (austria), *Geology*, *47*(1), 51–54, doi: 10.1130/G45281.1.

Grunnaleite, I., and A. Mosbron (2019), On the significance of salt Modelling—Example from modelling of salt tectonics, temperature and maturity around salt structures in southern north sea, *Geosciences Journal*, *9*(9), 363, doi: 10.3390/geosciences9090363.

Guilhaumou, N., J. C. Touray, V. Perthuisot, and F. Roure (1996), Palaeocirculation in the basin of southeastern france sub-alpine range: a synthesis from fluid inclusions studies, *Marine and Petroleum Geology*, *13*(6), 695–706, doi: 10.1016/0264-8172(95)00064-X.

Haccard, D., B. Beaudoin, P. Gigot, and M. Jordan (1989a), Notice explicative, carte géol. france (1/50 000), feuille la javie (918).

Haccard, D., B. Beaudoin, M. Lemoine, M. Lanteaume, P. Gigot, Y. Kerrien, J. Labourguigne, J. Manivit, and M. Jorda (1989b), Carte géologique de la france à 1/50000, feuille 918, la javie.

Handy, M. R., S. M. Schmid, R. Bousquet, E. Kissling, and D. Bernoulli (2010), Reconciling plate-tectonic reconstructions of alpine tethys with the geological–geophysical record of spreading and subduction in the alps, *Earth-Science Reviews*, *102*(3), 121–158, doi: 10.1016/j.earscirev.2010.06.002.

Hearon, T. E., IV, M. G. Rowan, K. A. Giles, R. A. Kernen, C. E. Gannaway, T. F. Lawton, and J. C. Fiduk (2015), Allochthonous salt initiation and advance in the northern flinders and eastern willouran ranges, south australia: Using outcrops to test subsurface-based models from the northern gulf of mexico, *AAPG bulletin*, *99*(02), 293–331, doi: 10.1306/08111414022.

Henry, D. G., I. Jarvis, G. Gillmore, and M. Stephenson (2019), Raman spectroscopy as a tool to determine the thermal maturity of organic matter: Application to sedimentary, metamorphic and structural geology, *Earth-Science Reviews*, *198*(102936), 102,936, doi: 10.1016/j.earscirev.2019.102936.

Herviou, C., P. Agard, A. Plunder, K. Mendes, A. Verlaguet, D. Deldicque, and N. Cubas (2022), Subducted fragments of the Liguro-Piemont ocean, western alps: Spatial correlations and offscraping mechanisms during subduction, *Tectonophysics*, *827*, 229,267, doi: 10.1016/j.tecto.2022.229267.

Hibsch, C., D. Kandel, C. Montenat, and P. Ott d'Estevou (1992), Evenements tectoniques cretaces dans la partie meridionale du bassin subalpin (massif Ventoux-Lure et partie orientale de l'arc de Castellane, SE France); implications geodynamiques, *Bulletin de la Société Géologique de France*, *163*(2), 147–158.

Hudec, M. R., and M. P. A. Jackson (2006), Advance of allochthonous salt sheets in passive margins and orogens, *AAPG Bulletin*, *90*(10), 1535–1564, doi: 10.1306/05080605143.

Hudec, M. R., T. P. Dooley, L. Burrel, A. Teixell, and N. Fernandez (2021), An alternative model for the role of salt depositional configuration and preexisting salt structures in the evolution of the southern pyrenees, spain, *Journal of Structural Geology*, *146*(104325), 104,325, doi: 10.1016/j.jsg.2021.104325.

Izquierdo-Llavall, E., A. Menant, C. Aubourg, J.-P. Callot, G. Hoareau, P. Camps, E. Péré, and A. Lahfid (2020), Preorogenic folds and Syn-Orogenic basement tilts in an inverted hyperextended margin: The northern pyrenees case study, *Tectonics*, *39*(7), e2019TC005,719, doi: 10.1029/2019TC005719.

Jackson, M. P. A., and M. R. Hudec (2017), *Salt Tectonics: Principles and Practice*, Cambridge University Press, doi: 10.1016/0040-1951(89)90177-7.

Jackson, M. P. A., and B. C. Vendeville (1994), Regional extension as a geologic trigger for diapirism, *GSA Bulletin*, *106*(1), 57–73, doi: 10.1130/0016-7606(1994)106<0057:REAAGT>2.3.CO;2.

Jensen, P. K. (1983), Calculations on the thermal conditions around a salt diapir, *Geophysical Prospecting*, *31*(3), 481–489, doi: 10.1111/j.1365-2478.1983.tb01064.x.

Jensen, P. K. (1990), Analysis of the temperature field around salt diapirs, *Geothermics*, *19*(3), 273–283, doi: 10.1016/0375-6505(90)90047-F.

Jourdan, S., M. Bernet, P. Tricart, E. Hardwick, J.-L. Paquette, S. Guillot, T. Dumont, and S. Schwartz (2013), Short-lived, fast erosional exhumation of the internal western Alps during the late early Oligocene: Constraints from geothermochronology of pro- and retro-side foreland basin sediments, *Lithosphere*, *5*(2), 211–225, doi: 10.1130/L243.1.

Jourdon, A., F. Mouthereau, L. Le Pourhiet, and J.-P. Callot (2020), Topographic and tectonic evolution of mountain belts controlled by salt thickness and rift architecture, *Tectonics*, *39*(1), 1–14, doi: 10.1029/2019tc005903.

Kalifi, A., C. Ribes, P. Dietrich, E. Dujoncquoy, J.-A. Muñoz, J.-P. Callot, and J.-C. Ringenbach (2023), Facies distribution along salt walls: The upper cretaceous mixed siliciclastic-carbonate deposits of the cotiella minibasins (southern pyrenees, spain), *Marine and Petroleum Geology*, *147*(105989), 105,989, doi: 10.1016/j.marpetgeo.2022.105989.

Kerckhove, C., and C. Lereus (1986), Un paléodiapir à coeur triasique resédimenté dans le crétacé du morgon (zone subbriançonnaise des nappes de l'Embrunais-Ubaye, zones internes des alpes occidentales françaises), *Comptes Rendus de l'Académie des Sciences de Paris*, *303*(20), 1813–1818.

Kerckhove, C., and C. Lereus (1987), Le détritisme des black shales crétacées du domaine subbriançonnais durancien. nouvelles données tirées du massif du morgon: un olistostrome à matériel triasique issu d'un diapir synsédimentaire, *Géologie Alpine*, *Mém. H.S.*, 235–245.

Kerckhove, C., and F. Thouvenot (2010), Notice explicative, carte géol. france (1/50 000), feuille allos (919).

Kley, J., and T. Voigt (2008), Late cretaceous intraplate thrusting in central europe: Effect of Africa-Iberia-Europe convergence, not alpine collision, *Geology*, *36*(11), 839–842, doi: 10.1130/G24930A.1.

Koyi, H. A., A. Ghasemi, K. Hessami, and C. Dietl (2008), The mechanical relationship between strike-slip faults and salt diapirs in the zagros fold–thrust belt, *Journal of the Geological Society*, *165*(6), 1031–1044, doi: 10.1144/0016-76492007-142.

Labaume, P., and A. Teixell (2020), Evolution of salt structures of the pyrenean rift (chaînons béarnais, france): From hyper-extension to tectonic inversion, *Tectonophysics*, *785*, 228,451, doi: 10.1016/j.tecto.2020.228451.

Labaume, P., M. Jolivet, F. Souquière, and A. Chauvet (2008), Tectonic control on diagenesis in a foreland basin: combined petrologic and thermochronologic approaches in the grès d'annot basin (late Eocene–Early oligocene, French–Italian external alps), *Terra nova*, *20*(2), 95–101, doi: 10.1111/j.1365-3121.2008.00793.x.

Lahfid, A., O. Beyssac, E. Deville, F. Negro, C. Chopin, and B. Goffé (2010), Evolution of the raman spectrum of carbonaceous material in low-grade metasediments of the glarus alps (switzerland), *Terra nova*, *22*(5), 354–360, doi: 10.1111/j.1365-3121.2010.00956.x.

Lanari, P., S. Guillot, S. Schwartz, O. Vidal, P. Tricart, N. Riel, and O. Beyssac (2012), Diachronous evolution of the alpine continental subduction wedge: Evidence from P–T estimates in the briançonnais zone houillère (france – western alps), *Journal of Geodynamics*, *56-57*, 39–54, doi: 10.1016/j.jog.2011.09.006.

Lapparent, d. A. F. (1940), Précisions nouvelles au sujet des diapirs de suzette (vaucluse) et de propiac (drôme), *Bulletin de la Société Géologique de France*, *s5-X*(1-2), 3–15.

Le Breton, E., S. Brune, K. Ustaszewski, S. Zahirovic, M. Seton, and R. D. Müller (2021), Kinematics and extent of the Piemont–Liguria basin – implications for subduction processes in the alps, *Solid earth*, *12*(4), 885–913, doi: 10.5194/se-12-885-2021.

Legeay, E., J.-C. Ringenbach, C. Kergaravat, A. Pichat, G. Mohn, J. Vergés, S. Kavak Kaan, and J.-P. Callot (2020), Structure and kinematics of the central sivas basin (turkey): salt deposition and tectonics in an evolving fold-and-thrust belt, *Geological Society, London, Special Publications*, *490*(1), 361–396, doi: 10.1144/SP490-2019-92.

Lemoine, M., T. Bas, A. Arnaud-Vanneau, H. Arnaud, T. Dumont, M. Gidon, M. Bourbon, P.-C. de Graciansky, J.-L. Rudkiewicz, J. Megard-Galli, and P. Tricart (1986), The continental margin of the mesozoic tethys in the western alps, *Marine and Petroleum Geology*, *3*(3), 179–199, doi: 10.1016/0264-8172(86)90044-9.

Li, X., L. Cai, S. Liu, and X. Li (2020), Thermal properties of evaporitic rocks and their geothermal effects on the kuqa foreland basin, northwest china, *Geothermics*, *88*(vember 2019), 101,898, doi: 10.1016/j.geothermics.2020.101898.

Liati, A., N. Froitzheim, and C. M. Fanning (2005), Jurassic ophiolites within the valais domain of the western and central alps: geochronological evidence for re-rifting of oceanic crust, *Contributions to mineralogy and petrology. Beitrage zur Mineralogie und Petrologie*, *149*(4), 446–461, doi: 10.1007/s00410-005-0658-7.

Lickorish, W. H., and M. Ford (1998), Sequential restoration of the external alpine digne thrust system, SE france, constrained by kinematic data and synorogenic sediments, *Geological Society, London, Special Publications*, *134*(1), 189–211.

Lopez-Mir, B., J. Anton Muñoz, and J. García Senz (2014), Restoration of basins driven by extension and salt tectonics: Example from the cotiella basin in the central pyrenees, *Journal of Structural Geology*, *69*(PA), 147–162, doi: 10.1016/j.jsg.2014.09.022.

Loprieno, A., R. Bousquet, S. Bucher, S. Ceriani, F. H. Dalla Torre, B. Fügenschuh, and S. M. Schmid (2011), The valais units in savoy (france): a key area for understanding the palaeogeography and the tectonic evolution of the western alps, *International Journal of Earth Sciences*, *100*(5), 963–992, doi: 10.1007/s00531-010-0595-1.

Manatschal, G., and O. Müntener (2009), A type sequence across an ancient magma-poor ocean–continent transition: the example of the western alpine tethys ophiolites, *Tectonophysics*, *473*(1), 4–19, doi: 10.1016/j.tecto.2008.07.021.

Manzotti, P., M. Ballèvre, P. Pitra, and F. Schiavi (2021), Missing lawsonite and aragonite found: P–T and fluid composition in meta-marls from the combin zone (western alps), *Contributions to mineralogy and petrology. Beitrage zur Mineralogie und Petrologie*, *176*(8), 60, doi: 10.1007/s00410-021-01818-0.

Mascle, G., H. Arnaud, G. Dardeau, J. Debelmas, P. Dubois, M. Gidon, d. P.-C. Graciansky, C. Kerckhove, and M. Lemoine (1986), Halocinèse précoce sur la marge téthysienne alpine : vers une réinterprétation des zones de gypse des alpes, *Comptes Rendus de l'Académie des Sciences de Paris*, *302*(II), 963–968.

Mascle, G., H. Arnaud, G. Dardeau, J. Debelmas, P. Delpech, P. Dubois, M. Gidon, P. Graciansky, C. Kerckhove, and M. Lemoine (1988), Salt tectonics, tethyan rifting and alpine folding in the french alps, *Bulletin de la Societe Geologique de France*, *8*(4), 747–758, doi: 10.2113/GSSGFBULL.IV.5.747.

McClay, K., J.-A. Muñoz, and J. García-Senz (2004), Extensional salt tectonics in a contractional orogen: A newly identified tectonic event in the spanish pyrenees, *Geology*, *32*(9), 737–740, doi: 10.1130/G20565.1.

Mello, U. T., G. D. Karner, and R. N. Anderson (1995), Role of salt in restraining the maturation of subsalt source rocks, *Marine and Petroleum Geology*, *12*(7), 697–716, doi: 10.1016/0264-8172(95)93596-V.

Michard, A., T. Dumont, L. Andreani, and N. Loget (2010), Cretaceous folding in the dévoluy mountains (subalpine chains, france): gravity-driven detachment at the european paleomargin versus compressional event, *Bulletin de la Société Géologique de France*, *181*(6), 565–581, doi: 10.2113/gssgfbull.181.6.565.

Miró, J., O. Ferrer, J. A. Muñoz, and G. Manastchal (2023), Role of inheritance during tectonic inversion of a rift system in basement-involved to salt-decoupled transition: analogue modelling and application to the Pyrenean–Biscay system, *Solid earth*, *14*(4), 425–445, doi: 10.5194/se-14-425-2023.

Motte, G., G. Hoareau, J.-P. Callot, S. Révillon, F. Piccoli, S. Calassou, and E. C. Gaucher (2021), Rift and salt-related multi-phase dolomitization: example from the northwestern pyrenees, *Marine and Petroleum Geology*, *126*, 104,932, doi: 10.1016/j.marpetgeo.2021.104932.

Nalpas, T., and J.-P. Brun (1993), Salt flow and diapirism related to extension at crustal scale, *Tectonophysics*, *228*(3), 349–362, doi: 10.1016/0040-1951(93)90348-N.

Negro, F., R. Bousquet, F. Vils, C.-M. Pellet, and J. Hänggi-Schaub (2013), Thermal structure and metamorphic evolution of the Piemont-Ligurian metasediments in the northern western alps, *Swiss Journal of Geosciences*, *106*(1), 63–78, doi: 10.1007/s00015-013-0119-7.

Parizot, O., D. F. Lamotte, and Y. Missenard (2023), A new look at old debates about the corbières (NE-Pyrenees) geology: salt tectonics and gravity gliding, *BSGF - Earth Sciences Bulletin*, *194*(6), 18, doi: 10.1051/bsgf/2023003/5832645/bsgf.

Pedrera, A., A. Ruiz-Constán, J. García-Senz, A. Azor, C. Marín-Lechado, C. Ayala, J. A. Díaz de Neira, and L. R. Rodríguez-Fernández (2020), Evolution of the South-Iberian paleomargin: From hyperextension to continental subduction, *Journal of Structural Geology*, *138*, 104,122, doi: 10.1016/j.jsg.2020.104122.

Pedrera, A., J. García-Senz, E. L. Pueyo, B. López-Mir, R. Silva-Casal, and J. Díaz-Alvarado (2023), Inhomogeneous rift inversion and the evolution of the pyrenees, *Earth-Science Reviews*, *245*(104555), 104,555, doi: 10.1016/j.earscirev.2023.104555.

Peel, F. J. (2014), How do salt withdrawal minibasins form? insights from forward modelling, and implications for hydrocarbon migration, *Tectonophysics*, *630*, 222–235, doi: 10.1016/j.tecto.2014.05.027.

Perthuisot, V., and N. Guilhaumou (1983), Les diapirs triasiques du domaine vocontien; phases diapiriques et hydrothermales en domaine perialpin, *Bulletin de la Societe Geologique de France*, *XXV*(3), 397–410, doi: 10.2113/GSSGFBULL.S7-XXV.3.397.

Peterson, K., and I. Lerche (1995), Quantification of thermal anomalies in sediments around salt structures, *Geothermics*, *24*(2), 253–268.

Philippe, Y., E. Deville, and A. Mascle (1998), Thin-skinned inversion tectonics at oblique basin margins: example of the western vercors and chartreuse subalpine massifs (SE france), *Geological Society, London, Special Publications*, *134*(1), 239–262, doi: 10.1144/GSL.SP.1998.134.01.11.

Plunder, A., P. Agard, B. Dubacq, C. Chopin, and M. Bellanger (2012), How continuous and precise is the record of *p–t* paths? insights from combined thermobarometry and thermodynamic modelling into subduction dynamics (schistes lustrés, w. alps), *Journal of Metamorphic Geology*, *30*(3), 323–346, doi: 10.1111/j.1525-1314.2011.00969.x.

Poprawski, Y., C. Basile, L. M. Agirrezabala, E. Jaillard, M. Gaudin, and T. Jacquin (2014), Sedimentary and structural record of the albian growth of the bakio salt diapir (the basque country, northern spain), *Basin Research*, *26*(6), 746–766, doi: 10.1111/bre.12062.

Poprawski, Y., C. Basile, Z. Cumberpatch, and A. Eude (2021), Mass transport deposits in deep-water minibasins: Outcropping examples from the minibasins adjacent to the bakio salt wall (basque country, northern spain), *Marine and Petroleum Geology*, *132*, 105,194, doi: 10.1016/j.marpetgeo.2021.105194.

Ramos, A., J. García-Senz, A. Pedrera, C. Ayala, F. Rubio, C. Peropadre, and J. F. Mediato (2022), Salt control on the kinematic evolution of the southern Basque-Cantabrian basin and its underground storage systems (northern spain), *Tectonophysics*, *822*, 229,178, doi: 10.1016/j.tecto.2021.229178.

Roca, E., O. Ferrer, M. G. Rowan, J. A. Muñoz, M. Butillé, K. A. Giles, P. Arbués, and M. de Matteis (2021), Salt tectonics and controls on halokinetic-sequence development of an exposed deepwater diapir: The bakio diapir, Basque-Cantabrian basin, pyrenees, *Marine and Petroleum Geology*, *123*, 104,770, doi: 10.1016/j.marpetgeo.2020.104770.

Rosenberg, C. L., N. Bellahsen, A. Rabaute, and J.-B. Girault (2021), Distribution, style, amount of collisional shortening, and their link to barrovian metamorphism in the european alps, *Earth-Science Reviews*, *222*, 103,774, doi: 10.1016/j.earscirev.2021.103774.

Rousset, C., A. Bambier, and C. Kerckhove (1983), Notice explicative, carte géologique de la france (1/50000), feuille seyne (894) - orléans, *Tech. rep.*, BRGM.

Rowan, M. G., and K. A. Giles (2021), Passive versus active salt diapirism, *AAPG bulletin*, *105*(1), 53–63, doi: 10.1306/05212020001.

Rowan, M. G., and B. C. Vendeville (2006), Foldbelts with early salt withdrawal and diapirism: Physical model and examples from the northern gulf of mexico and the flinders ranges, australia, *Marine and Petroleum Geology*, *23*(9), 871–891, doi: 10.1016/j.marpetgeo.2006.08.003.

Rowan, M. G., K. A. Giles, T. E. Hearon, IV, and J. C. Fiduk (2016), Megaflaps adjacent to salt diapirs, *AAPG bulletin*, *100*(11), 1723–1747, doi: 10.1306/05241616009.

Saspiturry, N., A. Lahfid, T. Baudin, L. Guillou-Frottier, P. Razin, B. Issautier, B. Le Bayon, O. Serrano, Y. Lagabrielle, and B. Corre (2020), Paleogeothermal gradients across an inverted hyperextended rift system: Example of the mauléon fossil rift (western pyrenees), *Tectonics*, *39*(10), doi: 10.1029/2020tc006206.

Schorn, A., and F. Neubauer (2014), The structure of the hallstatt evaporite body (northern calcareous alps, austria): A compressive diapir superposed by strike-slip shear?, *Journal of Structural Geology*, *60*, 70–84, doi: 10.1016/j.jsg.2013.12.008.

Schwartz, S., S. Guillot, B. Reynard, R. Lafay, B. Debret, C. Nicollet, P. Lanari, and A. L. Auzende (2013), Pressure–temperature estimates of the lizardite/antigorite transition in high pressure serpentinites, *Lithos*, *178*, 197–210, doi: 10.1016/j.lithos.2012.11.023.

Schwartz, S., C. Gautheron, L. Audin, T. Dumont, J. Nomade, J. Barbarand, R. Pinna-Jamme, and P. van der Beek (2017), Foreland exhumation controlled by crustal thickening in the western alps, *Geology*, *45*(2), 139–142, doi: 10.1130/G38561.1.

Sherkati, S., and J. Letouzey (2004), Variation of structural style and basin evolution in the central zagros (izeh zone and dezful embayment), iran, *Marine and Petroleum Geology*, *21*(5), 535–554, doi: 10.1016/j.marpetgeo.2004.01.007.

Sommaruga, A. (1999), Décollement tectonics in the jura forelandfold-and-thrust belt, *Marine and Petroleum Geology*, *16*(2), 111–134, doi: 10.1016/s0264-8172(98)00068-3.

Stampfli, G. M., and G. D. Borel (2002), A plate tectonic model for the paleozoic and mesozoic constrained by dynamic plate boundaries and restored synthetic oceanic isochrons, *Earth and planetary science letters*, *196*(1), 17–33, doi: 10.1016/S0012-821X(01)00588-X.

Stewart, S. A., and J. A. Clark (1999), Impact of salt on the structure of the central north sea hydrocarbon fairways, *Geological Society, London, Petroleum Geology Conference Series*, *5*(1), 179–200, doi: 10.1144/0050179.

Stewart, S. A., M. J. Harvey, S. C. Otto, and P. J. Weston (1996), Influence of salt on fault geometry: examples from the UK salt basins, *Geological Society, London, Special Publications*, *100*(1), 175–202, doi: 10.1144/GSL.SP.1996.100.01.12.

Strauss, P., P. Granado, and J. A. Muñoz (2021), Subsidence analysis of salt tectonics-driven carbonate minibasins (northern calcareous alps, austria), *Basin Research*, *33*(2), 968–990, doi: 10.1111/bre.12500.

Sue, C., P. Tricart, T. Dumont, and A. Pêcher (1997), Raccourcissement polyphasé dans le massif du pelvoux (alpes occidentales): exemple du chevauchement de socle de Villard-Notre-Dame, *Comptes Rendus De L Academie Des Sciences Serie Ii Fascicule A-sciences De La Terre Et Des Planetes*, *324*(IIa), 847–854, doi: 10.1016/S1251-8050(97)82520-7.

Tricart, P., P. van der Beek, S. Schwartz, and E. Labrin (2007), Diachronous late-stage exhumation across the western alpine arc: constraints from apatite fission-track thermochronology between the pelvoux and Dora-Maira massifs, https://www.lyellcollection.org/doi/10.1144/0016-76492005-174, doi: 10.1144/0016-76492005-174, accessed: 2024-2-12.

Valla, P. G., P. A. van der Beek, D. L. Shuster, J. Braun, F. Herman, L. Tassan-Got, and C. Gautheron (2012), Late neogene exhumation and relief development of the aar and aiguilles rouges massifs (swiss alps) from low-temperature thermochronology modeling and ^{4}He/^{3}He thermochronometry, *Journal of geophysical research*, *117*(F1), 1–23, doi: 10.1029/2011jf002043.

van Hinsbergen, D. J. J., T. H. Torsvik, S. M. Schmid, L. C. Maţenco, M. Maffione, R. L. M. Vissers, D. Gürer, and W. Spakman (2020), Orogenic architecture of the mediterranean region and kinematic reconstruction of its tectonic evolution since the triassic, *Gondwana Research*, *81*, 79–229, doi: 10.1016/j.gr.2019.07.009.

Vendeville, B. C., and M. P. A. Jackson (1992), The rise and fall of diapirs during thin-skinned extension, *AAPG bulletin*, *9*, 331–354.

Vergés, J., Y. Poprawski, Y. Almar, P. A. Drzewiecki, M. Moragas, T. Bover-Arnal, C. Macchiavelli, W. Wright, G. Messager, J.-C. Embry, and D. Hunt (2020), Tectono-sedimentary evolution of Jurassic–Cretaceous diapiric structures: Miravete anticline, maestrat basin, spain, *Basin Research*, *32*(6), 1653–1684, doi: 10.1111/bre.12447.

Vernet, J. (1966), Observations nouvelles sur le synclinal d'ailefroide et les bordures du massif du pelvoux en vallouise, *Trav. Lab. Géol. Grenoble*, *42*, 275–280.

Vernon, A. J., P. A. van der Beek, H. D. Sinclair, and M. K. Rahn (2008), Increase in late neogene denudation of the european alps confirmed by analysis of a fission-track thermochronology database, *Earth and planetary science letters*, *270*(3), 316–329, doi: 10.1016/j.epsl.2008.03.053.

Vizgirda, J., J. J. O'Brien, and I. Lerche (1985), Thermal anomalies on the flanks of a salt dome, *Geothermics*, *14*(4), 553–565, doi: 10.1016/0375-6505(85)90006-9.

Warren, J. K. (2006), *Evaporites:Sediments, Resources and Hydrocarbons*, Springer Berlin Heidelberg, doi: 10.1007/3-540-32344-9.

Wicker, V., and M. Ford (2021), Assessment of the tectonic role of the triassic evaporites in the north toulon fold-thrust belt, *Bulletin de la Societe Geologique de France*, *192*(51), 51, doi: 10.1051/bsgf/2021033.

Withjack, M. O., and S. Callaway (2000), Active normal faulting beneath a salt layer: An experimental study of deformation patterns in the cover sequence, *AAPG bulletin*, *84*(5), 627–651, doi: 10.1306/c9ebce73-1735-11d7-8645000102c1865d.

Zhuo, Q. G., F. W. Meng, M. J. Zhao, Y. Li, X. S. Lu, and P. Ni (2016), The salt chimney effect: delay of thermal evolution of deep hydrocarbon source rocks due to high thermal conductivity of evaporites, *Geofluids*, *16*(3), 440–451, doi: 10.1111/gfl.12162.